The eastern Kendeng Hills (Java, Indonesia) and the hominin-bearing beds of Mojokerto, a re-interpretation

Berghuis, H.W.K.; Kolfschoten, T. van; Adhityatama, S.; Troelstra, S.R.; Noerwidi, S.; Suriyanto, R.A.; ... ; Joordens, J.C.A.

Quaternary Science Reviews 295 (2022) 107692

Contents lists available at ScienceDirect

Quaternary Science Reviews

journal homepage: www.elsevier.com/locate/quascirev

The eastern Kendeng Hills (Java, Indonesia) and the hominin-bearing beds of Mojokerto, a re-interpretation

H.W.K. Berghuis [a, c, *], Thijs van Kolfschoten [a, d], Shinatria Adhityatama [l], S.R. Troelstra [g], Sofwan Noerwidi [e], Rusyad Adi Suriyanto [h], Unggul Prasetyo Wibowo [f], Eduard Pop [a, b], Iwan Kurniawan [i], Sander L. Hilgen [b, g], A. Veldkamp [j], Josephine C.A. Joordens [a, b, g, k]

[a] Faculty of Archaeology, Leiden University, P.O. Box 9514, Leiden, Netherlands
[b] Naturalis Biodiversity Center, P.O. Box 9517, Leiden, Netherlands
[c] Sealand Coastal Consultancy, van Baerlestraat 140, Amsterdam, Netherlands
[d] Institute of Cultural Heritage, Shandong University, 72 Binhai Highway, Qingdao, 266237, China
[e] Badan Riset Dan Inovasi Nasional, Organisasi Riset Arkeologi, Bahasa Dan Sastra, Jl. Condet Pejaten No.4, Jakarta, 12510, Indonesia
[f] Geological Museum, Jl. Diponegoro 57, Bandung, Jawa Barat, 40122, Bandung, Indonesia
[g] Faculty of Science, Vrije Universiteit, de Boelelaan, 1085, 1081HV Amsterdam, Netherlands
[h] Laboratory of Bioanthropology and Paleoanthropology, Universitas Gadjah Mada, Jl. Bulaksumur, Yogyakarta, Daerah Istimewa Yogyakarta, 55281, Indonesia
[i] Center for Geological Survey of Indonesia, Jl. Diponegoro 57, Bandung, Jawa Barat, 40122, Bandung, Indonesia
[j] Faculty ITC, University of Twente, P.O. Box 217, 7500 AE Enschede, Netherlands
[k] Faculty of Science and Engineering, Maastricht University, Kapoenstraat 2, 6211KW, Maastricht, Netherlands
[l] Griffith Centre for Social and Cultural Research, Griffith University, Gold Coast, QLD, Australia

ARTICLE INFO

Article history:
Received 2 March 2022
Received in revised form
28 July 2022
Accepted 31 July 2022
Available online 30 September 2022

Handling Editor: Dr Giovanni Zanchetta

Keywords:
Pleistocene
Stratigraphy
Sedimentology
Homo erectus
Vertebrate palaeontology
Volcanism
Sea-level changes
Tectonism
Brantas river
Sundaland

ABSTRACT

The eastern Kendeng Hills (Java, Indonesia) expose a 1000 m thick series that is used as a stratigraphic standard, representing the emergence of eastern Java from the sea. The fluvial top is rich in vertebrate fossils and yielded the Mojokerto (Perning) hominin skullcap, which is regarded as the earliest evidence of *Homo erectus* on Java, with age estimates ranging between 1.9 and 1.49 Ma. The series is commonly regarded as an uninterrupted record of coastal progradation. However, recent studies show that the emergence of eastern Java has been a complex process, under influence of tectonism, volcanism, sea-level fluctuations and fluvial dynamics, leaving a fragmented depositional record that varies from site to site. This is at odds with the prevailing stratigraphic practice of long-distance correlations and questions the existing interpretations of the eastern Kendeng reference sections. Here we present the results of a fieldwork-based re-interpretation of this key stratigraphic record, which we identified as the fill of a previously unrecognized Plio-Pleistocene embayment, surrounded by elongate uplift zones. Clinoform-bedded sandstones relate to a stage of explosive, high-silica volcanism, supplying large volumes of ash. The embayment fill is incised and covered by fluvial deposits, which we relate to the Middle Pleistocene Brantas. The fluvial strata have a cyclic build-up, probably representing sea-level controlled stages of aggradation and degradation. Based on a reconstruction of fluvial cycles, we provisionally link the conglomerate bed in which the Mojokerto *Homo erectus* was found to MIS14 (~550ka). We infer that the published radiometric ages derive from reworked volcanic clasts that make up this incisive fluvial lag and are not representative for the age of deposition. Our study places the eastern Kendeng series in a new landscape context and changes our view of the timing of hominin migration to Java.

1. Introduction

The eastern Kendeng (Fig. 1B) is a gentle fold belt rising up from the alluvial plains of eastern Java. It exposes a ca. 1000 m thick regressive series of Pliocene marine mudstones covered by

* Corresponding author. Aculty of Archaeology, Leiden University, P.O. Box 9514, Leiden, Netherlands.
E-mail address: h.w.k.berghuis@arch.leidenuniv.nl (H.W.K. Berghuis).

https://doi.org/10.1016/j.quascirev.2022.107692

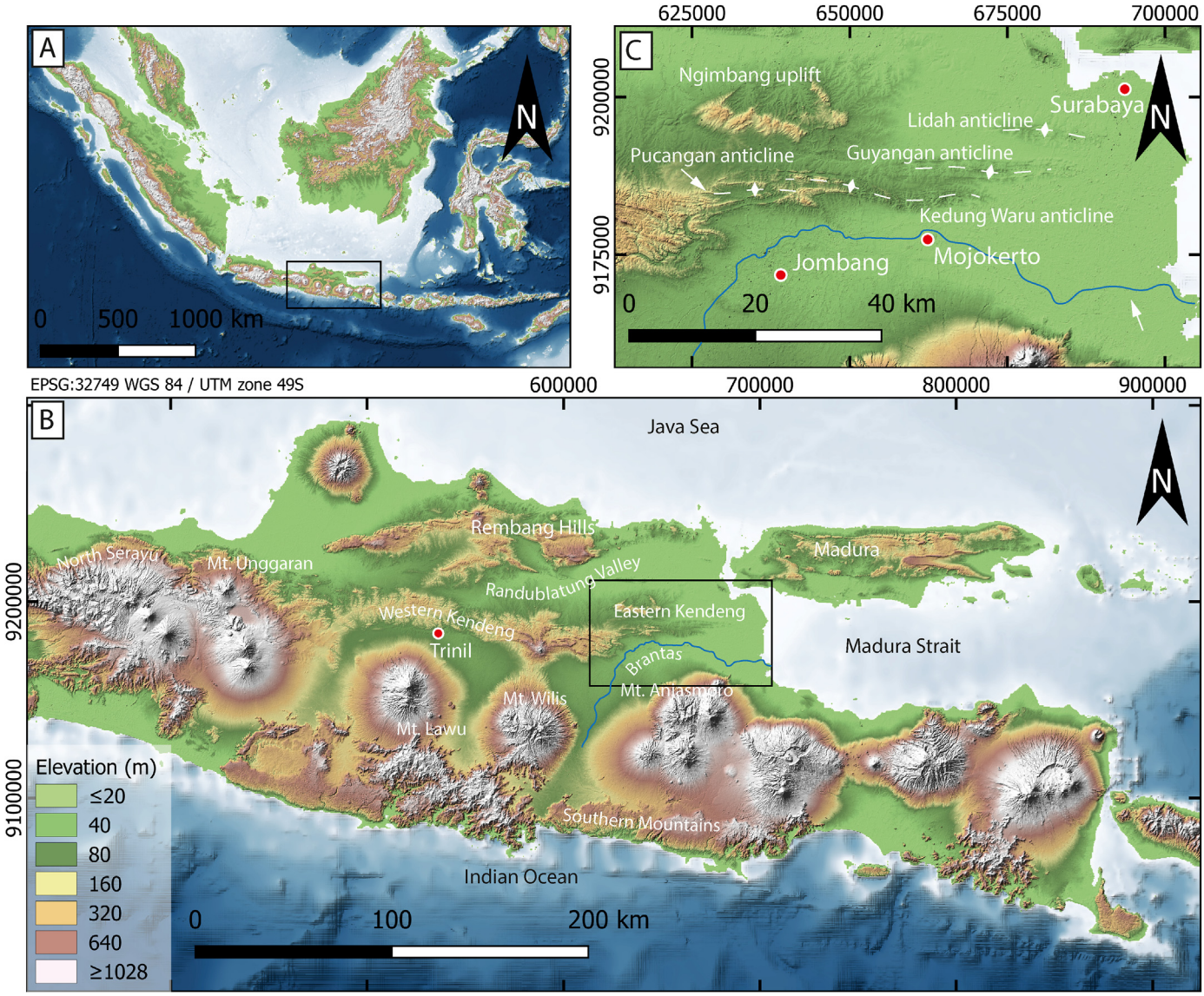

Fig. 1. A: The Indonesian archipelago with the study area on eastern Java. B: Eastern Java, the eastern Kendeng Hills and other sites mentioned in the text. C: The four anticlines making up the eastern Kendeng Hills., Map data: GEBCO (A, B, C) and ALOS (B, C).

alternating coastal and terrestrial strata of Pleistocene age. The area has special significance, as it holds the reference sections for the regional stratigraphy (Duyfjes, 1938) and it contains vertebrate fossils, which play a role in the regional biostratigraphy (De Vos and Sartono, 1982; Von Koenigswald, 1935). Moreover, a hominin skullcap, found in 1936 in Perning near Mojokerto (Von Koenigswald, 1936), is regarded as one of the oldest *Homo erectus* fossils of Java (Huffman, 2001; Morley et al., 2020; Morwood et al., 2003; Swisher et al., 1994)

Recent work on the hominin-bearing series of Trinil, ca. 100 km to the west, showed that the local depositional record, previously regarded as uninterrupted and directly related to the eastern Kendeng reference sections, has a complex build-up, of various depositional stages and hiatuses, reflecting the interplay of tectonism, volcanism, sea-level fluctuations and fluvial system dynamics (Berghuis et al., 2021). This complexity is reason to question the validity of the stratigraphic practice proposed by Duyfjes (1938, 1936), which is based on simple, long-distance correlations across eastern Java.

This new insight has implications for the eastern Kendeng stratigraphy. If this depositional record can no longer be regarded as the stratigraphic standard of a regional regression, what is its significance on a local scale, in terms of landscapes and depositional processes? And if this record also appears to be more complex than previously thought, how does this affect our ideas on the genesis and age of the Mojokerto hominin find site?

The objectives of our study are:

- To make a fieldwork-based re-inventory of the eastern Kendeng stratigraphic reference sections around Jombang and of the hominin-bearing series of Mojokerto;
- To re-interpret the eastern Kendeng series as a local stratigraphic record, representing local depositional processes and landscapes;
- To link the observed depositional record to published accounts on tectonism, volcanism and climate, and to the Pleistocene sea-level curve;
- To consider the implications of our findings for the age, depositional context and stratigraphic position of the vertebrate-

bearing beds of Mojokerto, focussing on the find site of the hominin skullcap.

2. Background

2.1. Geological setting

Java is located along the southern margin of the Sunda Shelf, directly north of the subduction zone where the Indian-Australian oceanic plate subducts under continental Sundaland. In the Early Miocene, most of present-day Java was part of a marine back-arc basin associated with an ancient volcanic arc in the south (Hamilton et al., 1979). In the Late Miocene, volcanism ceased over a length of ca. 200 km, corresponding to present-day eastern Java, probably caused by a buoyant part of oceanic crust that was not able to subduct (Hall and Spakman, 2015). The inactive volcanic arc eroded and changed into a submarine ridge with coral reefs (Smyth et al., 2008). In the adjacent back-arc basin, deposition changed from volcaniclastic turbidity currents to settling of calcareous ooze. In the Late Pliocene, the basin came under compression, possibly as a result of the resumption of active subduction in the south (Smyth et al., 2005). This resulted in uplift and the emergence of elongate hill ranges. The Rembang Hills and the Southern Mountains ridges were uplifted along pre-existing basement faults (Husein et al., 2015; Musliki and Saratman, 1996; Satyana et al., 2004), whereas the western Kendeng formed as a fold-and-thrust belt over the former back-arc basin (Genevraye and Samuel, 1972). In the Early Pleistocene, active volcanism returned, as a late response to resumed subduction, with the Wilis (Fig. 1B) as the first major eruption centre (Hartono, 1994).

Besides tectonism along the plate margin, the region has been subject to long-wavelength uplift and subsidence of the Sunda Shelf in relation to patterns of mantle flow (Zahirovic et al., 2016). Dynamic subsidence of the shelf prevailed during most of the Tertiary and Quaternary, although temporary disturbances of subduction caused intermittent stages of dynamic uplift. Seismic surveys of the submerged shelf revealed the existence of up to five marine sequences, overlying a basal Pleistocene unconformity, which are separated by internal unconformities, representing intermittent stages of fluvial incision (Alqahtani et al., 2015; Darmadi et al., 2007). This reflects a regime of alternating stages of submergence and emergence, following sea-level fluctuations, dating back to MIS11 (Sarr et al., 2019).

2.2. Hominin fossils and Von Koenigswald's vertebrate biostratigraphy

In the late 19th century, Dubois collected vertebrate fossils from fluvial strata along the southern foot slopes of the western Kendeng, notably around the village of Trinil (Fig. 1B). His finds include hominin fossils (Dubois, 1894), which form the type specimens of *Homo erectus* (Mayr, 1950; Meikle and Parker, 1994). Dubois regarded his vertebrate fossils as one faunal assemblage, which he referred to as the Trinil Fauna (Dubois, 1907). Later, vertebrate-bearing fluvial beds were also found in the eastern Kendeng north of Mojokerto (Cosijn, 1931, 1932). Von Koenigswald (1935, 1934) noted that these fossils differ from the Trinil Fauna and named this new assemblage the Jetis Fauna. According to his observations, the strata that yield the Jetis Fauna form a lower stratigraphic level than the fossil-bearing beds of Trinil. Using faunal characteristics, he assigned the Jetis Fauna to the Early Pleistocene and the Trinil Fauna to the Middle Pleistocene. Besides these two faunal units, Von Koenigswald defined a third: the Ngandong Fauna, referring to the fossil assemblage of a fluvial terrace near the village of Ngandong, discovered a few years earlier (e.g. Oppenoorth, 1932). For this faunal assemblage, Von Koenigswald assumed a Late Pleistocene age.

In 1936 a hominin skullcap was discovered in a conglomerate bed north of Mojokerto, near the village of Perning (Von Koenigswald, 1936). Its finding spot, within the stratigraphic range of the Jetis Fauna, implied an Early Pleistocene age, older than the hominin fossils from Trinil. The calvaria is regarded as a juvenile specimen (Storm, 1994) and often referred to as the 'Mojokerto child'.

2.3. Stratigraphy

In the 1930's, the Geological Survey of the Dutch East Indies started a geological mapping program of Java, assigning the geologist Duyfjes to map the Kendeng Hills and surroundings (Duyfjes, 1938). Duyfjes selected his reference sections in the eastern Kendeng north of Jombang (Fig. 1C), which he interpreted as an uninterrupted record of coastal progradation, driven by continuous volcanic supply that exceeded subsidence. The base of the exposed series (Fig. 2A) consists of calcareous and diatomaceous mudstones, which he referred to as the Kalibeng Formation. The lower boundary of this material is not exposed, but Duyfjes knew that in the western part of the hill range the calcareous mudstones are underlain by bedded marine claystones with Miocene foraminifera. Consequently, he assigned the Kalibeng Formation to the Pliocene.

The mudstones are overlain by several hundred meters of marine clays, which Duyfjes named the Pucangan Formation, with an assumed Early Pleistocene age. Duyfjes noted that the clays, which are omnipresent in the eastern Kendeng, wedge out toward the west. Around Trinil, they are absent and instead the calcareous Kalibeng Formation is directly overlain by volcanic breccias. Referring to their similar stratigraphic position, and to his model of uninterrupted sedimentation and regional subsidence, Duyfjes correlated the breccias of Trinil with the marine clays of Jombang, naming the breccias of Trinil the volcanic Facies of the Pucangan Formation.

Duyfjes observed the marine clays to be overlain by bedded coastal sandstones and fluvial sandstones and conglomerates. He linked these strata to the breccias of Trinil and added them to the Volcanic Facies of the Pucangan Formation, describing a landscape of andesitic lahars and fluvial re-distribution to a muddy coast in the northeast. Referring to Von Koenigswald's (1935, 1934) vertebrate biostratigraphy, Duyfjes drew a unit boundary in the fluvial series. He assigned the lower part of this series, containing the Early Pleistocene Jetis Fauna, to the Pucangan Formation. For the overlying fluvial strata, containing the Middle Pleistocene Trinil Fauna, he defined a separate unit: the Kabuh Formation. This stratigraphic subdivision worked out well for the Trinil area. Here, the volcanic breccias, regarded as the Pucangan Formation, are overlain by fluvial sandstones, which yielded Dubois' Trinil Fauna and therefore 'by definition' form the Middle Pleistocene Kabuh Formation (Duyfjes, 1936).

Duyfjes' stratigraphy (Fig. 2A) is essentially a chronostratigraphic framework, combining strata of different facies in stratigraphic units based on assumed age relations. Extrapolations (he spoke of 'parallelization') form a recurrent aspect in his stratigraphy. Even in his reference section, the position of the boundary between the Pucangan and Kabuh Formations is determined by extrapolations with fossil finds from a wide area.

According to Duyfjes' model, the prolonged conditions of regional subsidence finally changed to uplift and folding in the late Middle Pleistocene, after the deposition of the Kabuh Formation, forming the Kendeng Hills.

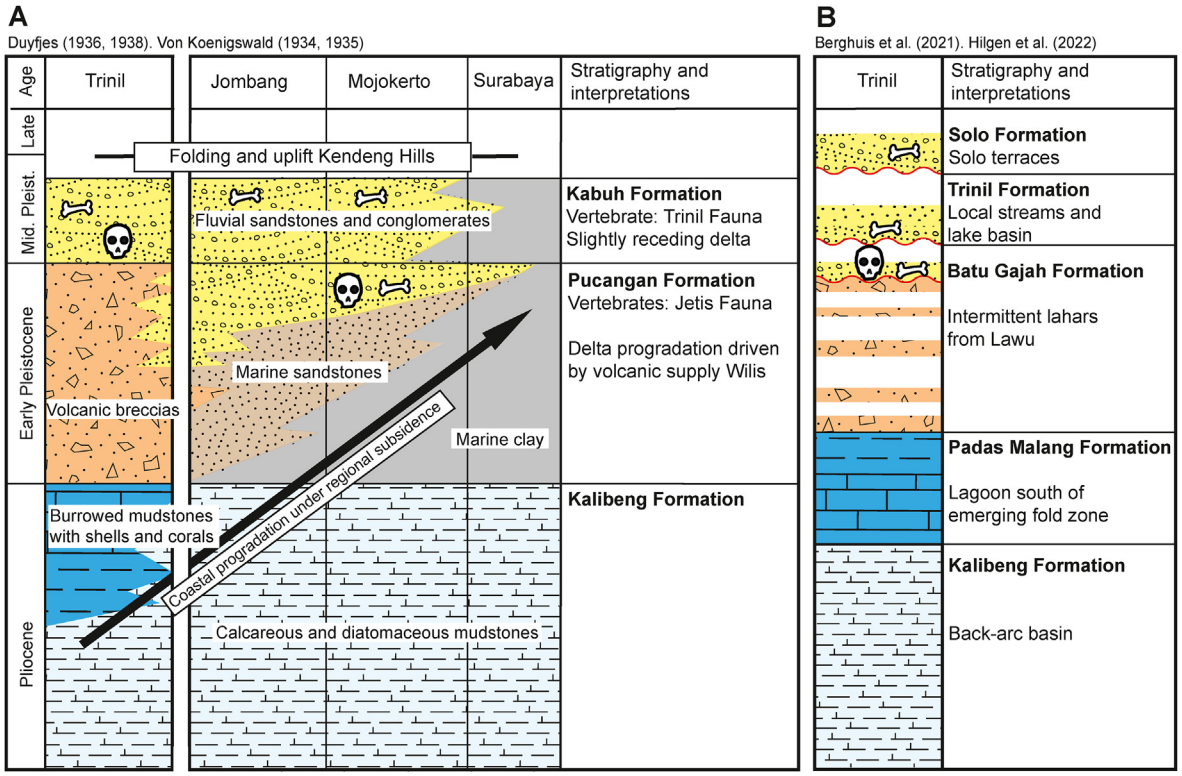

Fig. 2. A: Stratigraphy and correlations of the 1930's. The framework consists of chronostratigraphic units and is based on a landscape model of coastal progradation driven by volcanic supply. B: Revised stratigraphy and interpretations of the hominin-bearing series of Trinil. Note: simplified representation, for detailed information on hiatuses, incisions and paleosols refer to the original papers.

2.4. Cracks in the stratigraphic model

Recent insight in eastern Java tectonism (Section 2.1) indicates that Duyfjes' model of uninterrupted sedimentation under prolonged subsidence, followed by late Middle Pleistocene folding is too simple. The emergence of eastern Java has been influenced by more complex tectonism, forming several elongate uplift zones and leaving intermediate areas as deposition centers. Folding and emergence of the western Kendeng dates from the Late Pliocene and left a shallow basin along its southern flanks. Trinil is located in the marginal area between this uplifted ridge and the adjacent basinal area. Our recent work around Trinil (Berghuis et al., 2021) revealed a complex fill of intermittent lahars, separated by long hiatuses in which the area was subject to weathering and incision, or covered with coastal marshes. The fluvial strata along the top of this series represent several stages of local drainage systems, which were finally captured by the Solo (Fig. 2B).

This shows that the eastern Java depositional record is more complex than previously understood and reflects alternating stages of deposition, non-deposition, erosion and reworking, most of which have local relevance only. This raises questions about the validity of the previous correlations. For Trinil, a local stratigraphic framework has been defined (Fig. 2B). The same has been done earlier in Sangiran (Itihara et al., 1994). However, for the remaining part of eastern Java, Duyjes' units have remained commonly used.

2.5. Revised vertebrate biostratigraphy

Questions have also arisen on the validity of the biostratigraphic framework and its implications for dating and demarcating stratigraphic units. De Vos and Sartono (1982) re-evaluated the work of Dubois and Von Koenigswald and concluded that their faunal assemblages were made up of mixed finds with poorly documented (stratigraphic) provenance. They proposed a revision of the faunal subdivision, distinguishing between the Trinil HK (= *Hauptknochenschicht* or Main Bone Bed) Fauna, the Kedung Brubus Fauna and the (unchanged) Ngandong Fauna. The Trinil HK Fauna derives from a specific stratigraphic level within the Trinil find site and contains an assemblage that is considered as homogeneous (Van den Bergh, 1999). It is poor in species and may represent an early-stage island setting of eastern Java. The Kedung Brubus Fauna is a richer fauna, pointing to a subsequent influx of species via a land connection with the Asian mainland. De Vos and Sartono (1982) assigned the fossils from Mojokerto to the Kedung Brubus Fauna, suggesting that the Perning skullcap is younger than the Trinil skullcap.

Van den Bergh et al. (2001) provisionally dated the faunal units to 0.9 Ma (Trinil HK Fauna) and 0.8–0.7 Ma (Kedung Brubus Fauna). The revised faunal units and their ages have become generally accepted. Nevertheless, Duyfjes' Pucangan and Kabuh Formations, which were based on the former biostratigraphy, have remained in use, including their assumed (older) ages.

2.6. Recent developments with regard to the vertebrate biostratigraphy

The Ngandong Fauna derives from a single river terrace that has been dated to 140–92 ka (Rizal et al., 2020). Recent work in Trinil has shown that the Hauptknochenschicht or Main Bone bed is made up of two channel fills, which date to 830–773 ka and 540–380 ka respectively (Hilgen, under review; Pop, under review). The age of the oldest channel is close to the age as proposed by Van den Bergh et al. (2001). The younger channel incises into the older channel, and its vertebrate fossils may partly or largely be reworked.

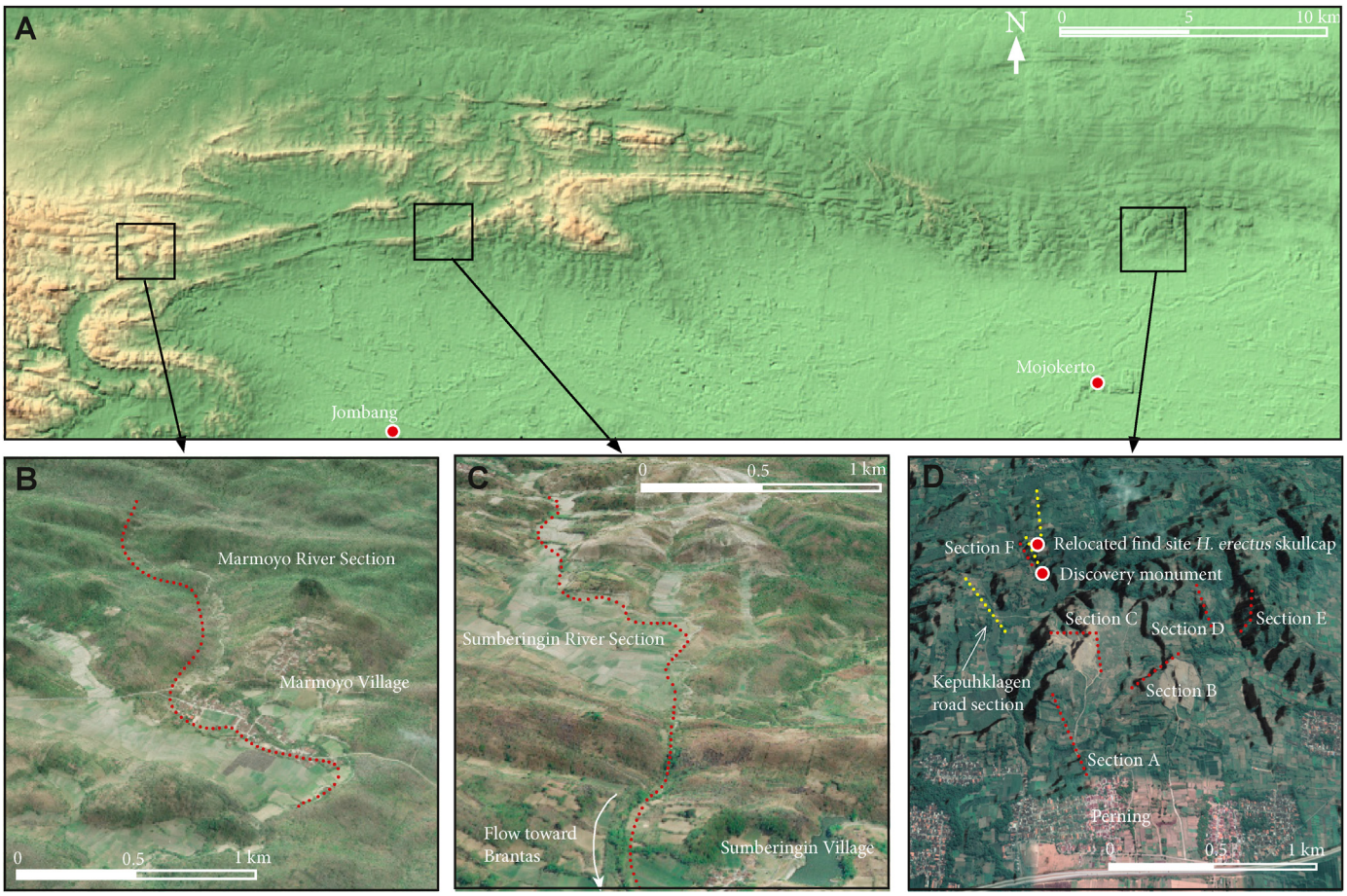

Fig. 3. A: The eastern Kendeng and the studied sections north of Jombang and Mojokerto. B: Marmoyo River Section (Jombang area). C: Sumberingin River Section (Jombang area). D: Kepuhklagen Road Section near Perning, quarry sections and *Homo erectus* find site (Mojokerto area).

Although the age and background of the Ngandong and Trinil HK Faunas are nowadays better understood, this does not account for the Kedung Brubus Fauna. This assemblage derives from a poorly studied fluvial interval of >200 m thick (Duyfjes, 1936), which may very well have a more complex build-up than commonly assumed.

2.7. Age of the perning skull

K/Ar and Ar/Ar-dating of pumice from the hominin-bearing bed of Perning (Mojokerto) yielded ages of 1.9 ± 0.5 Ma (Jacob and Curtis, 1971) and 1.81 ± 0.04 Ma (Swisher et al., 1994). These old ages, older than any other known Asian *Homo erectus*, were regarded as evidence of early hominin migration out of Africa. The ages are in line with the former (bio)stratigraphic frameworks Von Koenigswald and Duyfjes and seem to contradict with the revised biostratigraphy of De Vos and Sartono (1982). Morwood et al. (2003) obtained an age of 1.49 ± 0.13 Ma using fission track analyses on multiple zircons from pumice gravel, which still places the fossil among the oldest hominin remains of Java (Matsu'ura et al., 2020), but within the generally accepted age range of Asian of *Homo erectus* (Dennell, 2009). For the interpretations of the available radiometric ages it is noted that the K/Ar and Ar/Ar ages represent crystallization ages of hornblende crystals. This crystallization may already take place in the magma chamber, possibly resulting in a radiometric age that precedes the eruption age. Fission track ages represent the time elapsed since the zircon grains were last exposed to temperatures above 240 °C. These ages therefore probably more closely represent the actual eruption age.

The published radiometric ages have been assumed to approximate the age of fluvial deposition, referring to Duyfjes' landscape model of Early Pleistocene volcanic supply and quick eastward fluvial redistribution. De Vos and Sondaar (1994) and Langbroek and Roebroeks (2000) suggested that the sampled pumice consists of reworked volcanic material and that fluvial deposition may be younger. Morwood et al. (2003) provided additional sedimentological justification for their claim of contemporary volcanism, stating the dated material was sampled from a horizon consisting largely of granular pumice, forming a ca. 15 cm thick layer with great lateral continuity.

Paleomagnetic measurements of the depositional record of Mojokerto indicated a dominance of reversed polarities in the basal marine strata, changing to predominantly normal and intermediate polarities around the transition to the terrestrial, fossil-bearing strata (Hyodo et al., 1993; Sartono, 1981). Sartono (1981) related this polarity change to the Brunhes-Matuyama boundary. However, Hyodo et al. (1993) continued their measurements upwards through the stratigraphy and again found predominantly reversed and intermediate polarities. The authors correlated the interval of normal polarities, including the fossiliferous beds, with the Jaramillo Subchron. Swisher et al. (1994) correlated this interval with the Olduvai Subchron, referring to their older radiometric ages, whereas Morwood et al. (2003) correlated it with the Sangiran excursion, a temporary swing of declination between the Olduvai

and Jaramillo Subchrons (Hyodo et al., 1992). Huffman (2001) regarded the normal polarities as a result of recent overprint and not indicative of age.

3. Methods

During field campaigns in 2018 and 2019 we studied several river and quarry sections through the anticlines north of Jombang and Mojokerto (Figs. 1C and 3). We followed the routes of the researchers of the 1930's, and added new observations from recent quarries. All sections were measured, described and photographed. Interpretations have been based on published facies models, notably Tucker (1985) for shallow marine carbonates, Elliott (1986) for shallow marine clastic deposits, Bhattacharya (2006) for deltaic and Miall (2014, 1996) for fluvial deposits. The petrography of sand and conglomerate beds was determined in the field by hand lens and described semi-quantitatively. Special attention has been paid to unconformities in the form of (subaqueous) scour surfaces, fluvial incisions or paleosols, representing hiatuses in the depositional record. The successions between such unconformities are referred to as depositional sequences.

Fossil molluscs and corals were collected, described and photographed in the field. Identification has been carried out at Naturalis Biodiversity Center, based on descriptions and photographs, mostly up to genus level. Vertebrate fossils have not been excavated.

For the lower part of the studied section, published foraminiferal analyses are available (Berghuis et al., 2019). For the upper part of the section, additional samples were prepared and investigated for microfossils at the Vrije Universiteit, Amsterdam. To retrieve the foraminifera, the samples were placed in a cup with hot water and a detergent. After soaking for some hours, the samples were washed over a >63 μm sieve and dried on a hotplate. Subsequently, the dry residues were studied under a binocular microscope. Total occurrences of planktonic and benthic foraminifera were listed as poor, moderately rich or rich. The faunal analysis was carried out semi-quantitatively, with occurrences per species listed as scattered, common or abundant. Diatoms, mainly occurring in the unstudied <63 μm fraction, were not included in our study.

4. Sedimentology

Six genetically significant facies associations (FA) were identified, based on texture, composition, sedimentary structures, (micro)fauna and stratigraphic position. The six FA represent depositional settings ranging from open marine to coastal and terrestrial.

4.1. FA1: Open marine, bathyal depths

4.1.1. Description

White, planar laminated or platy diatomaceous mudstones (Fig. 4, photo 1) alternating with white, massive calcareous mudstones (Fig. 4, photo 2). The massive calcareous facies contains varying amounts of admixed detrital clay and may locally be referred to as calcareous-argillaceous mudstones, with a light grey color (Fig. 4, photo 3).

The diatomaceous facies is poor in foraminifera, with a planktonic/benthic-ratio > 99% (=P/B-ratio). Planktonic foraminifera are represented by scattered occurrences of *Globorotalia tumida*, *Globigerinoides trilobus, Globigerinoides ruber* and *Sphaeroidinella dehiscens.* Benthic foraminifera are extremely scarce or absent. For diatoms, reference is made to Reinhold (1937), who referred to the diatomaceous strata of the eastern Kendeng as the Pengampon Formation.

The massive calcareous facies is rich in well-preserved foraminifera, with a P/B-ratio of ~99%. Planktonic foraminifera are dominated by *Globorotalia menardii* (dex.), *Neogloboquadrina pseudopima, G. trilobus, Globigerina bulloides, G. tumida* and *G. ruber.* Scattered benthic foraminifera consist of *Gyroidina* sp., *Uvigerina peregrina, Pullenia bulloides, Bulimina marginata* and *Cibicidoides wuellerstorfii.*

4.1.2. Interpretation

The mudstones of FA1 represent open marine conditions. Benthic foraminiferal species, as well as the P/B-ratio of over 99%, point to bathyal depths. The laminated diatomaceous facies represents stages of eutrophication, blooming phytoplankton and reduced oxygen conditions, which Berghuis et al. (2019) relate to upwelling. The massive calcareous mudstones represent intervening stages of reduced phytoplankton growth, normal oxygen conditions and a rich planktonic foraminiferal fauna, dominated by tropical species. Admixed argillaceous material reflects a low supply of fine terrestrial detritus.

4.2. FA2: Mud-dominated outer shelf

4.2.1. Description

Dark grey, slightly bluish, massive clay (Fig. 4, photo 4). The material is moderately rich in fine organic matter and practically devoid of admixed sand or silt. Carbonate content is very low. Locally the clay contains concentric calcareous concretions (diameter up to ~10 cm).

The clay is moderately rich in foraminifera, with a P/B-ratio of ~95%. Planktonic foraminifera consist primarily of *G. menardii* (sin. and dex.), *N. pseudopima*, *Neogloboquadrina humerosa*, *G. trilobus*, *G. tumida* and *G. ruber*. The benthic assemblage is represented by scattered occurrences of *Lenticulina* sp., *Ammonia supera*, *Eponides* sp., *Pseudorotalia gaimardii, B. marginata, Hoeglundia elegans, Uvigerina* sp., *Laticarinina pauperata* and *Gyroidina* sp..

4.3. Interpretation

This FA is regarded as extensively bioturbated marine mud. The composition of the material points to a rich supply of terrestrial weathering products and a setting in the proximity of an emerged landmass. The benthic assemblage is dominated by shelf species, but also contains deeper water species such as *Uvigerina* sp., *L. pauperata*, *Gyroidina* sp. and *B. marginata*, suggesting upper bathyal to outer shelf depth conditions. Benthic species as *Ammonia supera* and *Pseudorotalia gaimardii* point to low dissolved oxygen concentrations at the seabed, which probably relate to microbial respiration of accumulated organic matter. Microbial respiration probably also caused the slightly bluish color of the clays and the occurrence of concentric calcareous concretions (e.g. Sellés-Martínez, 1996) The concretions occur on distinct levels and probably reflect episodes of reduced sedimentation, allowing for concretion growth over a longer period. The moderately rich occurrence of planktonic foraminifera shows that normal oxygen conditions prevailed in the water column.

4.4. FA3 Mud-dominated shallow marine

4.4.1. Description

Light grey, bedded marine clay with sandy laminae and thinly interlayered clay-sand alternations (Fig. 4, photo 7). The material is moderately rich in organic matter. Sandy laminae and thicker sand beds are fine-grained and dominated by fine shell debris, admixed with lithic grains (andesite and pumice) and occasional glauconite. The material contains sparse vertical burrows. Sand beds may have

Fig. 4. Selected photographs of the Jombang section. 1: Diatomaceous mudstones (FA1). 2: Calcareous mudstones (FA1). 3: Argillaceous-calcareous mudstones (FA1). 4: Massive marine clays (FA2). 5: Paleosol capping the massive marine clays. 6: Transgressive lag over the paleosol, with shell fragments and andesite gravel. 7: Shallow marine clay-sand alternations (FA3). 8: Shell beds capping coastal progradation cycles (FA3). 9: Idem, close up. 10: Clinoform-bedded tuffaceous sand alternating with laminated mud (FA4). 11: Clinoform-bedded tuffaceous sand (FA4), overview of sets separated by internal unconformities (Kabuh quarry).

wavy or lenticular bedding structures. Locally, channelled sand beds occur, with a fill of coarse shell fragments, fine gravel (mainly moderately rounded andesite clasts) and clay pebbles. Occasional interbeds are found of massive, blocky-structured, dark grey clays, which may contain fine root traces and dispersed fine pyrite crystals.

The material is moderately rich in foraminifera, with a P/B-ratio of ~75%. Planktonic foraminifera are poorly preserved and often have broken or iron-stained tests. *G. trilobus, Dentoglobigerina altispira, G. menardii* (dex), *Pulleniatina obliquilocuta, G. ruber*,

G. tumida and *Sphaeroidinella subdehiscens* are among the most common species. Benthic foraminifera are represented by rich occurrences of *Pseudorotalia coinoides, Asterorotalia trispinosa, Elphidium* sp. and the larger species *Amphistegina lessonii* and *Gypsina* sp..

The material contains cemented sand beds (up to 15 cm thick) rich in bivalve fragments (Fig. 4, photo 8–9), consisting of Pectinidae indet, Carditidae indet., *Ostrea* sp., and *Timoclea* sp.. The fragments have rounded edges and are arranged in laminae, with the shells mostly in a convex-upwards position.

4.5. Interpretation

FA3 is indicative of shallow marine conditions under a rich supply of fine clastic material. The preservation of bedding structures is indicative of a relatively high sedimentation rate. Clays with fine sandy laminae represent inner shelf, subtidal depths, with sandy laminae reflecting storms or episodes of high fluvial discharge. Wavy and lenticular-bedded clay-sand alternations point to tidal currents. Channelled incisions with coarse fills rich in shell fragments represent tidal or estuarine channels. Interbeds of massive organic clays with fine pyrite crystals are indicative of coastal marshes, with thorough bioturbation and intermittent flooding (Pons et al., 1982).

The bivalve species are indicative of relatively turbulent conditions. The rounded shell fragments point to transport. Their occurrence as laminae with a convex-upward orientation reflects winnowing, either under shallow subtidal conditions or under intertidal conditions. The calcite-cementation of some of the shell beds may relate to early diagenesis by intermittent subaerial exposure, pointing to an origin as intertidal bars.

The benthic foraminiferal assemblage is characteristic of coastal or estuarine conditions. The planktonic foraminifera represent open water conditions and must have been transported to the coast by waves and tidal currents. An abundance of broken and iron-stained planktonic tests indicates that the assemblage contains reworked specimens, probably supplied as a terrestrial weathering product.

4.6. FA4 Ash-dominated deltas

4.6.1. Description

Yellowish grey, fine-grained tuffaceous sandstones, forming dm-scale bedding structures separated by mud drapes or thicker, laminated mud layers (Fig. 4, photo 10). The beds are normal graded and have an indistinct, parallel stratification. Grains consist of monocrystalline feldspars, vitric grains, lithic pumice and scarce fine shell fragments. Thicker sand beds often have a composite build-up of several amalgamated, graded sand layers.

The sandstone beds may be horizontally bedded, but more often form clinoforms with a depositional dip of 5–15°, locally reaching even steeper inclinations of up to 25° (Fig. 4, photo 11; Fig. 5, photos 9 and 11). Dipping beds often have a slightly incisive base, covered with a veneer of coarse tuffaceous sand with fine pumice gravel and clayey rip-up clasts, quickly grading upwards into fine tuff. The bedding planes are often distorted by soft sediment deformation or slumping. Horizontally-bedded sandstones are dominated by fine tuff and have more prominent clayey interbeds (Fig. 5, photo 1).

The material is poor in foraminifera, mostly with abraded and poorly preserved tests. Benthic species include *B. marginata*, *A. supera*, *Cibicides* sp., *Amphistegina* sp.. Among the fragmented planktonic tests are *Neogloboquadrina* sp. and Sphaeroidinella sp..

4.7. Interpretation

FA4 represents deltaic depositional conditions under a high supply of volcanic ash, pointing to explosive volcanism in the hinterland. Clinoform-bedded sands with thin clayey interbeds were deposited on the dipping delta slope. Tuffaceous sand beds with thicker clayey interbeds and a low or indistinct depositional dip may represent a pro-delta setting or a setting along a shallow, low-gradient coast.

The normal grading and slightly incisive base of the foresets reflect delta progradation by intermittent turbidity currents. The dominance of silt and fine-grained sand and the scarcity of well-rounded, coarser material points to supply by sediment-laden rivers, with a high suspension load and relatively low bed-load transport. Possibly, the sand beds represent short episodes of extreme run-off, which caused incoming high-density river water to plunge beneath the seawater, flowing over the delta slope as turbidity currents (e.g. Mulder and Syvitski, 1995; Zavala, 2020). Such situations may be related to flash floods in the upstream reach of the river and may have been amplified by ebb currents in the river mouth. Also, soft sediment deformation and slumps hint at episodes of high sediment supply and destabilization of the delta slope. Clay laminae, alternating with fine-sandy foresets, represent settling from a buoyant plume in front of the river mouth during intervening stages. The rhythmic build-up of fine sandy foresets and mud drapes may reflect seasonal variation in river discharge.

The scarce, abraded and broken foraminifera are regarded as reworked tests and must have been supplied to the delta by the river. Note that the benthic species form an unusual assemblage of bathyal and coastal species, which also points to reworking.

4.8. FA5 Sheltered interdistributary bays and coastal lakes

4.8.1. Description

Greenish grey, massive, siltstones with marine molluscs (Fig. 5, photo 6). The sediment is thoroughly bioturbated, locally preserving vertical burrows. The material consists of tuffaceous grains (vitric particles and monocrystalline feldspars), fine shell debris and calcareous grains and is admixed with calcareous mud. The material is rich in gastropods (*Turitella* sp., *Architectonica* sp., Tonnidae indet., *Strombus* sp., *Oliva* sp., *Ficus* sp., *Natica* sp.) and bivalves (Veneridae indet, Pectenidae indet., *Anadara* sp., *Ostrea* sp.). The shells are found either fragmented or in-situ. Fragmented shells have sharp edges and occur dispersed through the sediment. The material contains scattered free-living corals *Goniopora stokesi*.

The material is poor in foraminifera, dominated by benthic species as *Amphistegina* sp. and *Ammonia* sp.. Planktonic foraminifera are scarce and are represented by unidentifiable, abraded and broken specimens.

Loacally, the mollusc-rich siltstones are sharply overlain by finely laminated clays (Fig. 5, photos 4, 5 and 7), without traces of incision or weathering that might point to a depositional hiatus. The clay is made up of light and dark grey laminae, forming distinct and laterally continuous couplets. The dark laminae have a thickness of 2–3 mm and consist of clay with fine decomposed plant fragments and may contain imprints of leave fragments. The light laminae range in thickness between 1 and 4 mm and are composed of clay with admixed fine ash. Remarkably, the laminated clays are devoid of marine molluscs, which forms a great contrast with the underlying mollusc-bearing siltstones. Except for extremely scarce occurrences of broken foraminiferal tests, the material is also devoid of foraminifera.

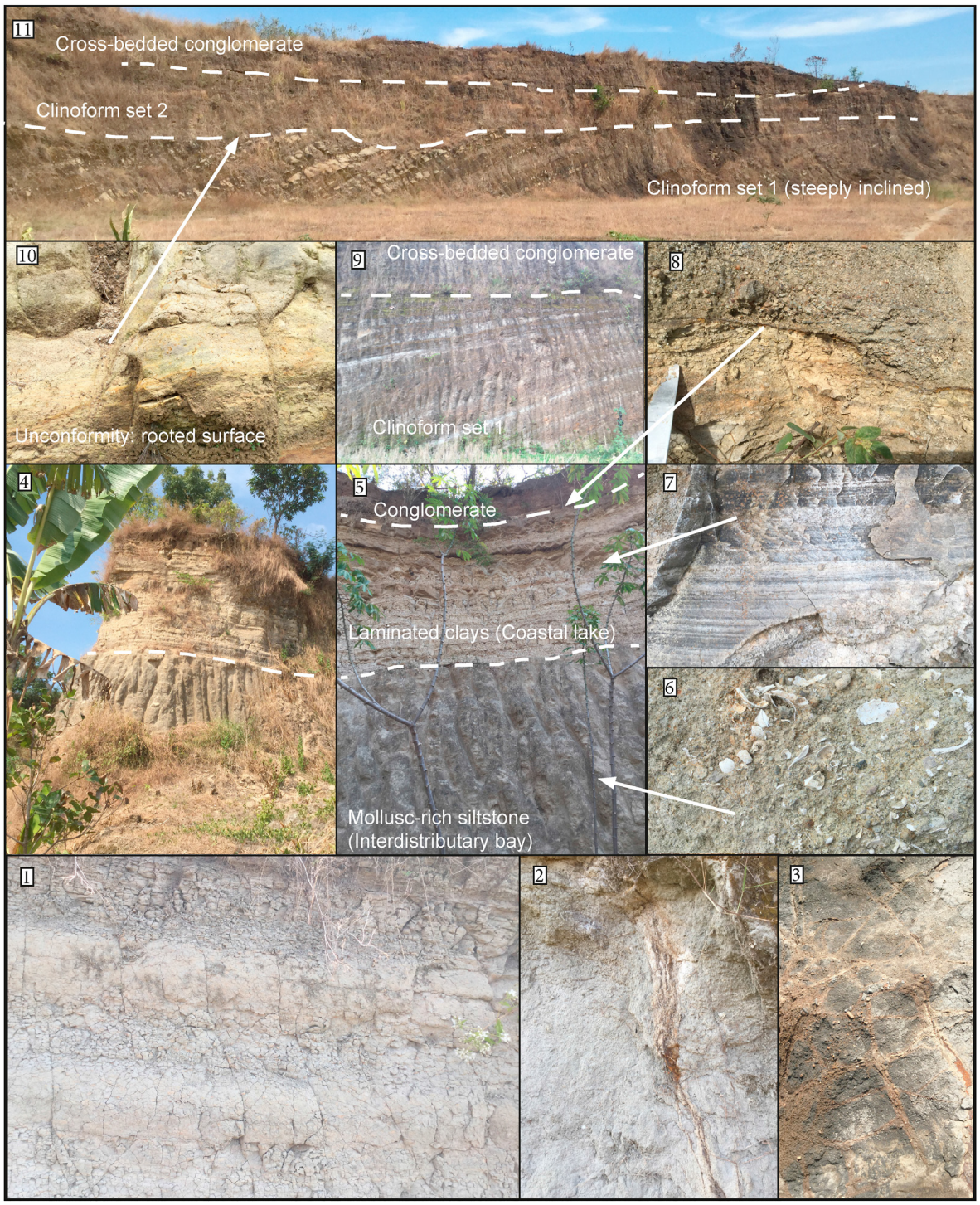

Fig. 5. Selected photographs of the Mojokerto section. 1: Bedded tuffaceous sand and laminated mud (FA4) forming base of the exposed section. 2: Tree root, paleosol overlying basal series of bedded tuffaceous sand. 3: Mud cracks, same level as photo 2.4: Mollusc-rich siltstones (interdistributary bay) sharply overlain by laminated clays (coastal-lake facies) (FA5). 5: Idem, laminated clays (FA5) are incised and overlain by cross-bedded conglomerate bed (FA6). 6: Close-up mollusc-rich siltstones (FA5). 7: Close-up laminated clays (FA5). 8: Close-up incisive contact between laminated clays (FA5) and cross-bedded conglomerate (FA6). 10: Horizon with fine root traces marking unconformity between clinoform-bedded sets. 11: Two clinoform-bedded sets separated by unconformity, set 2 is incised and overlain by cross-bedded conglomerates.

4.9. Interpretation

The burrowed, mollusc-rich mudstones represent a sheltered, shallow marine setting. In section 6.5 we will see that this sheltered environment is closely related to the landscape of ash-dominated deltas as described in section 4.4, suggesting a background as interdistributary bays.

The rich mollusc assemblage, dominated by gastropods, represents a low-energy and clear-water habitat, with a depth range of 5–20 m. Also the benthic fauna dominated by *Amphistegina* sp. and

the scattered free-living corals point to shallow, clear-water conditions. Scarce abraded tests of planktonic foraminifera are regarded as reworked specimens, probably supplied by rivers.

Dispersed shell fragments with sharp edges do not show signs of significant transport or wave action. Fragmentation is probably related to predation and compaction. In-situ molluscs point to episodic rapid burial. The ash-dominated composition of the sediment points to terrestrial supply from a volcanic hinterland.

The sharp transition to laminated clays represents an abrupt change to stagnant-water conditions. The sudden disappearance of marine molluscs and foraminifera suggests that the former lagoon has become isolated from the sea, changing the area into a coastal lake. The preservation of fine laminae suggests anoxic bottom conditions. Anoxic conditions in coastal lakes are often related to salt bottom waters, leading to stratification and inefficient mixing of the water column (Zolitschka et al., 2015).

4.10. FA6 Meandering and anastomosing rivers

4.10.1. Description

Reddish-brown conglomerates, yellowish-grey cross-bedded and planar bedded sandstones and dark grey organic clays, forming fining-upward sequences with a preserved thickness of up to 8 m. A sequence has a channelled or planar erosive base, covered with ca. 1.5 m of trough cross-bedded conglomerate (Fig. 6 photos 1–3 and 8–9). The conglomerate has a matrix of cemented coarse sand (feldspars, pyroxenes, hornblendes, lithic pumice and andesite) and contains moderately to well-rounded gravel (2–5 cm), with a polymict composition of pumice, dacite and andesite. Clayey rip-up clasts (up to 10 cm) are common. The conglomerate contains scattered, well-mineralized, disarticulated and often fragmented vertebrate bones. This basal lag is overlain by several meters of medium to fine-grained sandstones. Trough cross-bedding structures may be found in the lower few meters (Fig. 6, photo 10), but more often the sand is planar bedded and alternates with thin clay layers with fine root traces or thin paleosols with a blocky texture, root traces and fine carbonate concretions (Fig. 6, photos 5 and 7). Frequently, thicker (~1 m) interbeds occur of massive, dark grey clay rich in organic matter (Fig. 6, photo 6), containing in-situ molluscs (*Corbicula* sp., *Geloina* sp.).

4.11. Interpretation

The erosive lower boundary of a fluvial sequence, overlain by a gravelly lag, points to incision by a laterally mobile gravel-bed river, suggesting meandering conditions. The polymict gravel derives from the foot of the Wilis and Anjasmoro volcanoes and the rounding reflects stable bed-load transport. The overlying fining-upward sequence generally represents meandering conditions, with trough cross-bedded point-bar deposits overlain by floodplain soils. However, stacking of planar-bedded fine-grained sand and interbedded floodplain soils forms a distinctive feature of the fluvial sequences, pointing to repeated burial of the floodplain by wash-overs or avulsions from the main channel. Overbank deposition and high floodplain sedimentation rates are indicative of anastomosing conditions and are generally associated with rapid base-level rise (Makaske, 2001). Also the occurrence of thicker clayey interbeds points to this direction, as anastomosed rivers have low-lying, saucer-shaped floodplains, which frequently develop into wetlands. The in-situ molluscs in these clay layers represent a fresh or brackish water habitat. Probably, the fluvial fining upward cycles reflect an initial erosive stage, under meandering conditions, followed by an aggradational stage, under (partly) anastomosing conditions.

5. The depositional records of Jombang and Mojokerto

5.1. Jombang

North of Jombang, the Pucangan anticline rises up from the Brantas floodplain (Fig. 1). Duyfjes (1938) selected river sections through the south flank of this anticline, as a reference for his Kendeng stratigraphy. We focussed on the Marmoyo and Sumberingin Sections (Fig. 3), as these two sections cover the entire depositional series that makes up this flank of the anticline. Moreover, a published foraminiferal biostratigraphy provides detailed age control of the marine strata making up the base of these sections (Berghuis et al., 2019). The Marmoyo and Sumberingin Sections reach a total thickness of ca. 1000 m (Figs. 7 and 8).

The base of the series, exposed in the core of the anticline, consists of calcareous and diatomaceous mudstones (FA1), dating from the Early Pliocene. The material is generally very low in admixed detrital clay, but around 290 m above the base of the section, clay content increases, changing the sediment into calcareous-argillaceous mudstones. Foraminiferal age markers indicate that this facies change dates to ~3.8 Ma.

Ca. 430 m above the base of the section this material quickly grades into plastic marine clays (FA2). An array of planktonic age markers provides good age control over this part of the section (Fig. 7), indicating that this prominent facies change dates to 3.0 Ma.

The massive clays reach a thickness of 250 m. The base of the clays still contains a characteristic tropical planktonic foraminiferal assemblage. However, higher up a strong decline of *G. tumida*, a coiling change from dextral to sinistral in *G. menardii* and the appearance of *Neogloboquadrina* cf. *pachyderma* point to slightly cooler water conditions. These fauna changes are regionally used to mark the Plio-Pleistocene boundary (Blow, 1969; Bolli et al., 1989). The massive clays are capped with a ca. 1.5 m thick weathering profile of stiff, crumbly, red-colored clay with fine iron concretions (Fig. 4, photo 5). This layer is truncated and covered with a lag of coarse sand with shell fragments and fine andesitic gravel (Fig. 4, photo 6). The lag is overlain by shallow marine clay-sand alternations with shell fragments (FA3), reaching a thickness of 120 m. This shallow marine series can be roughly subdivided in three superimposed coarsening upwards sequences, grading from clay with fine sandy laminae to clay-sand alternations with wavy and lenticular bedding structures. Toward the top of these sequences, calcite-cemented shell lags occur (Fig. 4, photos 7–9), as well as dark grey organic clay layers with fine pyrite crystals. Planktonic age control is lost, as most age-relevant species are thermocline-dwelling and require sufficient water depth. Moreover, the material contains abundant red-stained planktonic foraminifera with eroded tests, which probably derive from eroded older strata, further complicating age determinations. For example, *D. altispira, S. subdehiscens* and dextrally coiled *G. menardii,* all present in the shallow marine strata, are Pliocene species for which extinctions were found lower in the depositional record (Fig. 7).

At ~810 m above the base of the section, the shallow marine clays quickly grade into fine-grained, bedded tuffaceous sandstones (FA4). Today the sand quarry of Kabuh, ca. 1.5 km west of the Sumberingin Section, provides excellent exposures of this material (Fig. 4, photo 10–11). The bedding planes dip ca. 40° (N145S). Reducing this value with the tectonic dip, which is ca. 30° (N170E),

Fig. 6. Selected photographs of the Mojokerto section (continued). 1: First conglomerate lag, base of the fluvial series (FA6), oldest preserved stage of the ancient Brantas. 2: Idem, close-up. 3: Idem. 4: Monument commemorating *Homo erectus* find, placed on basal conglomerate bed. Later reconstructions indicated that the actual find site is the second conglomerate bed. 5: Stacked floodplain deposits with root traces (FA6). 6: Vertisol in floodplain series (FA6). 7: Stacked floodplain soils, covered with overbank deposits (FA6). 8: Incision covered with second conglomerate lag (FA6). 9: Close-up second conglomerate lag. 10: Cross-bedded sand overlying second conglomerate lag (FA6). 11: Incision and third conglomerate lag. 12: Bedded organic clays and transition to marine interval. 13: Bedded marine claystones and sand with sparse burrows and mollusc fragments (FA3). 14: Alternating marine claystones and incisive fluvial sandstones, top of the section (FA3 and FA6).

leaves an eastward-directed dip of 10–15°, which we regard as a sedimentary, clinoform-related dip. The series reaches a total thickness of ca. 150 m and is built up of superimposed deltaic progradation sequences, forming sets of clinoforms with a thickness ranging between 10 and 50 m. Sets of clinoforms are separated by unconformities marked with burrows or fine root traces, often covered with a lag of fine shell fragments and clay pebbles.

The Kabuh quarry does not expose the top of the clinoform-bedded series, but in the Sumberingin River Section, the series can be traced southwards toward the footslopes of the hill range

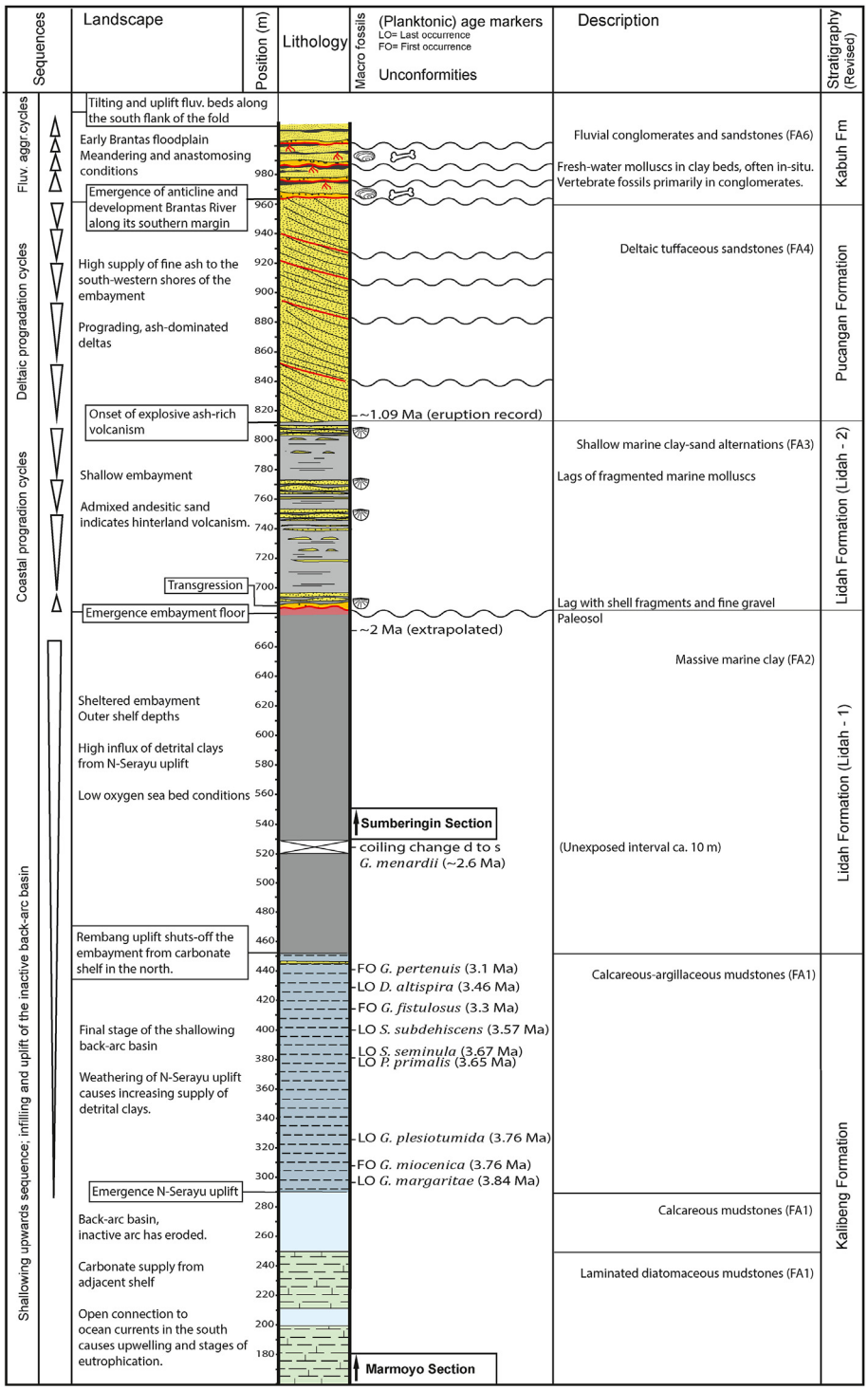

Fig. 7. Composite stratigraphic column of the Pucangan anticline north of Jombang, based on the Marmoyo and Sumberingin River Sections. See separate legend. Planktonic foraminiferal age markers are based on Berghuis et al. (2019). Age estimate of ~1.09 Ma is based on a provisional link with the Wilis eruption record (Hartono, 1994). FA = Facies Association, see section 4. Revised unit definitions based on this paper.

(Fig. 8A). Here, the tuffaceous clinoform-bedded series is truncated by a channelled erosion surface, covered with a trough-crossbedded, reddish-brown conglomerate lag. This basal lag is overlain by a ~25 m thick, poorly exposed fluvial series (FA6), made up of three or four stacked fining-upward sequences, each with an incisive base covered with a conglomerate lag.

5.2. Mojokerto

The succession as exposed around Jombang can be traced eastward toward the Kedung Waru anticline north of Mojokerto (Fig. 1). This low and smooth fold contains the bone-bearing fluvial strata that form the type locality of Von Koenigswald's Jetis Fauna and yielded the Perning skullcap. Duyfjes (1938), Huffman and

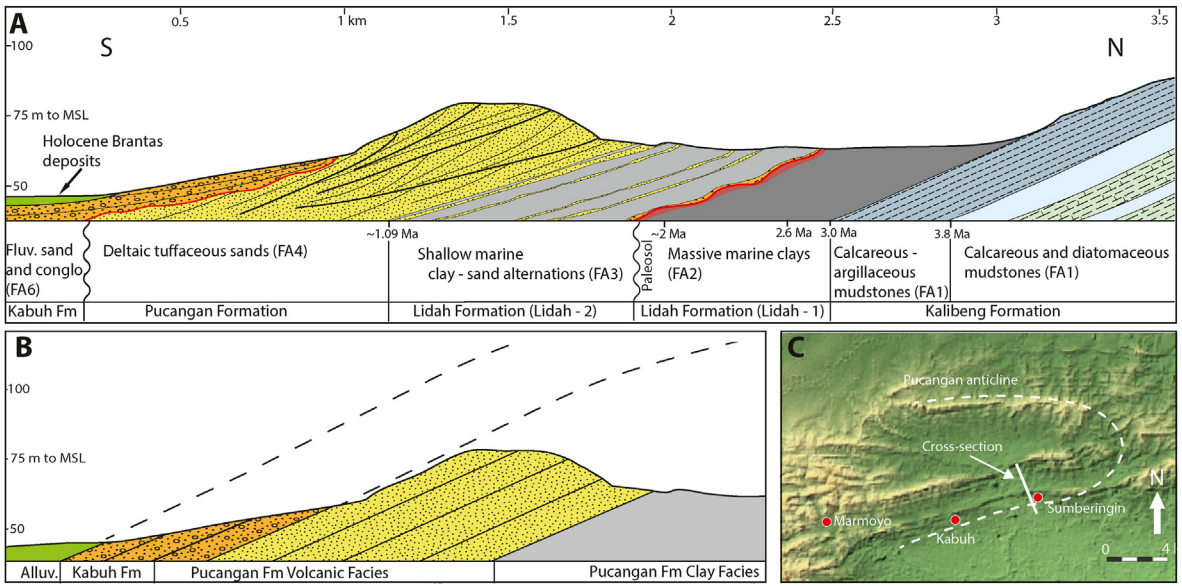

Fig. 8. A: Schematic cross-section over the south flank of the Pucangan anticline north of Jombang. FA = Facies Association, see section 4. The fluvial strata making up the southern foot slopes of the anticline postdate initial folding. They are part of a younger fluvial valley fill and have become tilted and uplifted along the margin of the anticline by continued folding. B: Previous interpretation and unit definition (Duyfjes, 1938), in which the series forms an uninterrupted record of coastal progradation and pre-dates folding. Fluvial strata along the southern flank do no re-appear along the northern flank, but were correlated with marine deposits which were regarded of equal age and which were referred to as the marine facies of the Kabuh Formation. C: Location of the cross-section.

Zaim (2003) and Morley et al. (2020) described a section through the anticline along Kepuhklagen Road. We restudied this section by combining detailed sections of the sand quarries north of the village of Perning, directly east of the Kepuhklagen Road, offering an unprecedented insight into the geological build-up of the anticline (Fig. 3D). Six quarry sections (sections A to F) were studied, representing a combined thickness of 54 m (Figs. 9 and 10).

The strata as exposed in the Kedung Waru anticline form the stratigraphic equivalent of the top of the Jombang section. Shallow marine clays (FA3) make up the core of the Kedung Waru anticline. The material is exposed several kilometers east of the Kepuhklagen Road Section. Duyfjes (1938) also reported the material in exposures along Kepuhklagen Road, but this could not be confirmed during our field studies.

In the studied quarry sections of Perning - Kepuhklagen, the lowest exposed stratigraphic level consists of the bedded, fine-grained tuffaceous sandstones (FA4). The material makes up the base of quarry sections A and E (Fig. 10) and reaches a maximum exposed thickness of 5 m. The tuffaceous beds have prominent clayey interbeds (Fig. 5, photo 1) and do not have a significant clinoform-related dip. The strata are capped with a thin weathering profile, with shrinkage cracks and root traces (Fig. 5, photos 2–3). In quarry section A, two paleosols are found at this level, separated by several meters of shallow marine sands and clays with shell fragments and interbedded organic clays with fine root traces and pyrite crystals, with a facies similar to FA3, but with a more tuffaceous composition of the sand grains.

The paleosol is overlain by ca. 8 m of burrowed, ash-rich siltstone, rich in marine molluscs (FA5), which is sharply overlain by ca. 5 m of finely laminated clays (FA5) (Fig. 5, photos 4–7). In quarry section A, several meters of organic clays with root traces are found between the mollusc-rich siltstones and the laminated clays.

The laminated clays become slightly sandier toward the top and are overlain by fine-grained bedded tuffaceous sandstones (FA4), with a prominent depositional dip of ca. 25° (N40E), corrected for tectonic dip (Fig. 5, photos 9 and 11). Moreover, the steeply dipping clinoforms have a parallel, mostly undistorted bedding structure. Remarkably, the tuffaceous beds in this part of the section are devoid of shell fragments or foraminifera, a feature that was also noted by Huffman and Zaim (2003). The steeply dipping clinoforms form one single set. In some of the larger quarries, a second set can be observed, separated from the underlying set by an unconformity with fine, red-colored grass-root traces (Fig. 5, photos 10 and 11). The clinoforms in the overlying set have a depositional dip of ca. 15° (N35E) and contain low quantities of shell debris and scarce foraminifera, mostly as abraded or broken tests. The clinoforms can be traced along the quarry sides for hundreds of meters and locally wedge out into the surrounding laminated clays (Fig. 10).

The tuffaceous clinoforms are truncated by a channelled erosion surface (Fig. 5, photos 9 and 11), locally leaving only several meters of the clinoform-bedded sands or even cutting down into the underlying laminated clays. Where the deltaic sands wedge out, the erosive surface incises the laminated clay (Fig. 5, photos 5 and 8). The erosion surface is covered with a cross-bedded, cemented conglomerate bed (Fig. 6, photos 1–3), which is overlain by (planar) bedded, medium to fine-grained sand with interbedded paleosols and clays (FA6). Several meters higher a new erosion surface is found, which is slightly channelled but in general forms a planar erosion surface that can be traced over long distances. It is covered with a cemented conglomerate lag, forming a plateau at ca. 59 m + MSL along the southern and central part of the hill range, which is around the axis of the anticline (Fig. 11A). The erosion surface truncates the underlying fluvial sequence with its more irregular erosive base. Locally, the younger erosion surface directly truncates the deltaic beds (Fig. 10, section B). Although the 59 m + MSL plateau resembles a fluvial terrace, remnants of overlying deposits indicate that it has formed by erosion of overlying, less consolidated material. This material again consists of bedded fluvial sand with interbedded floodplain soils and organic clays (FA6). It is exposed in isolated hills along the core of the anticline, reaching ca. 79 m + MSL. Moreover, it forms elongate crests of northward-dipping strata along the north flank of the anticline. Another prominent abrasion surface, again with a lag of cross-bedded conglomerate, marks the base of a third fining-

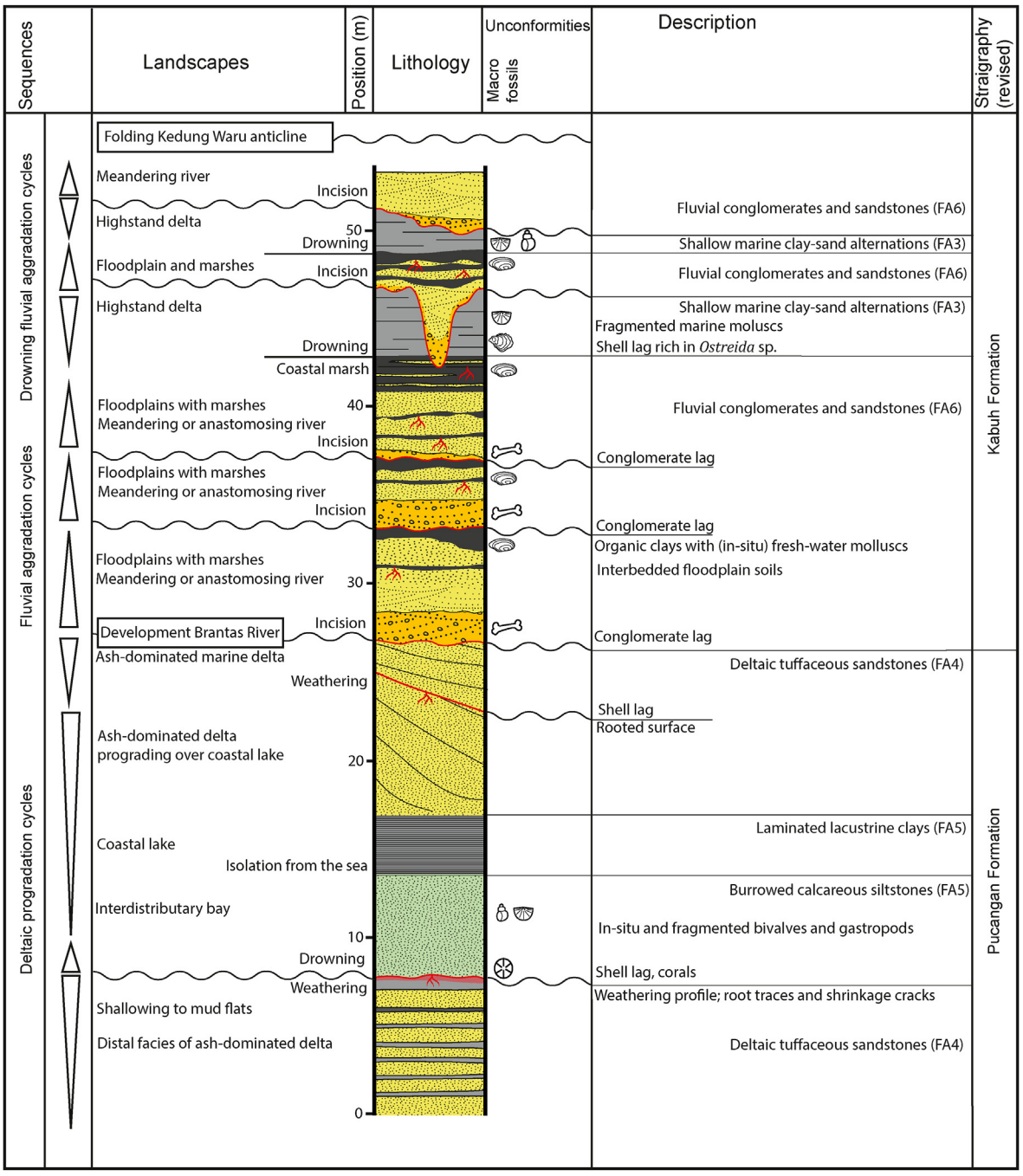

Fig. 9. Composite stratigraphic column of the Kedung Waru anticline north of Mojokerto, based on quarry sections east of Kepuhklagen Road. FA = Facies Association. Revised unit definitions based on this paper. See separate legend for Figs. 7 and 9.

upward sequence. This sequence grades into bedded organic clays (Fig. 6, photo 12), which are sharply overlain by an unstructured lag of rounded shell fragments, dominated by *Ostrea* sp.. It marks the transition to bedded claystones, with thin sandy interbeds and sparse marine molluscs (FA3) (Fig. 6, photo 13). The marine interval, which reaches a thickness of ca. 5 m, is deeply incised by channels with a fill of (cross-)bedded conglomerates and sandstones (FA6), which is again overlain by shallow marine clay-sand alternations (FA3). This marine interval is once again fluvially incised and the moderately cemented fluvial fill of this incision (FA6) caps the isolated hilltops (Fig. 6, photo 14).

Upon comparing our field descriptions with the published studies of this site, we found that the internal structure of the Kedung Waru anticline is different than previously thought. Its south flank is largely missing, probably due to faulting, which changes the perspective of the local stratigraphy (Fig. 11C). Fortunately, it is possible to trace back most of the previous field observations. Von Koenigswald (1935, 1934) and Duyfjes (1938, 1936) used two mollusc-bearing intervals as field markers, which the latter referred to as mollusc beds 2 and 3 (Fig. 11B). Mollusc bed 2 is the burrowed siltstone interval (FA5) within the ash-dominated deltaic series (FA4). Mollusc bed 3 is the shallow marine interval (FA3) near the top of the section, interbedded between fluvial strata. Von Koenigswald based his Jetis Fauna on vertebrate fossils

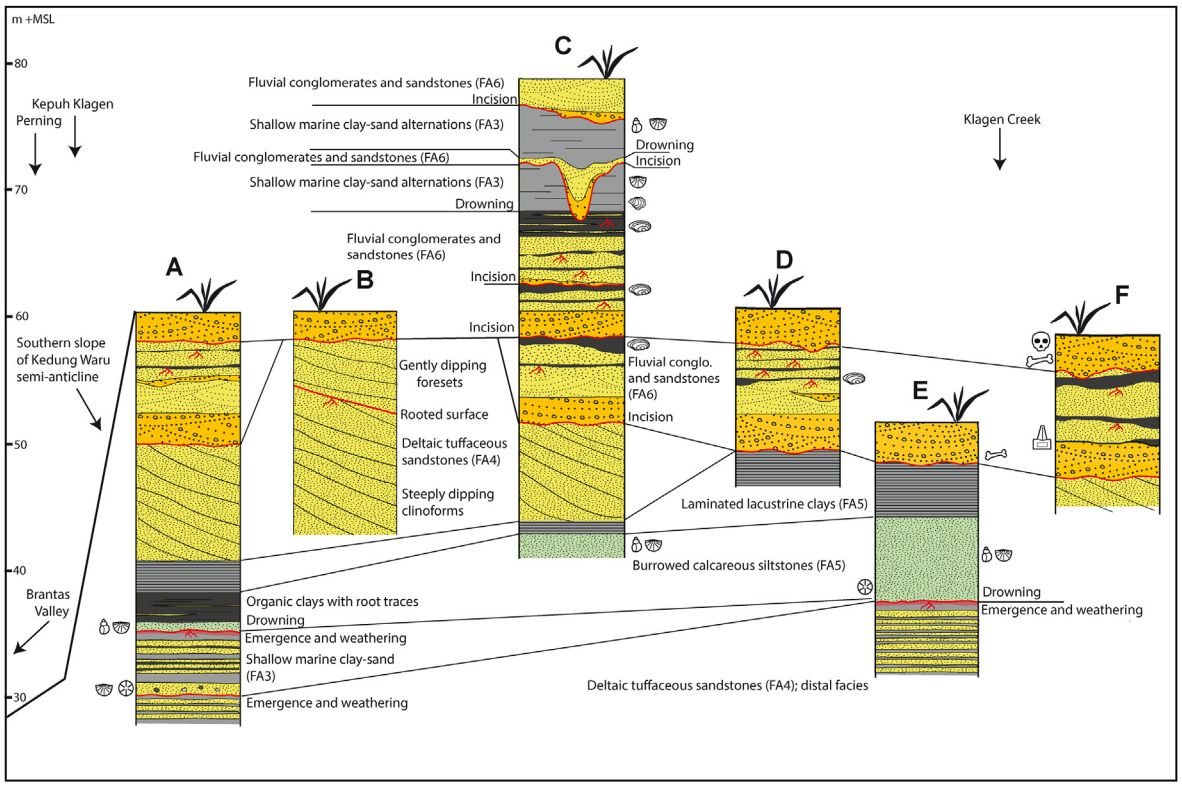

Fig. 10. Quarry sections of the Kedung Waru anticline north of Jombang, east of Kepuhklagen Road. FA = Facies Association, see section 4. For details, see composite stratigraphic column (Fig. 7). Location of the quarry sections is indicated in Fig. 3D. Legend: see Fig. 9.

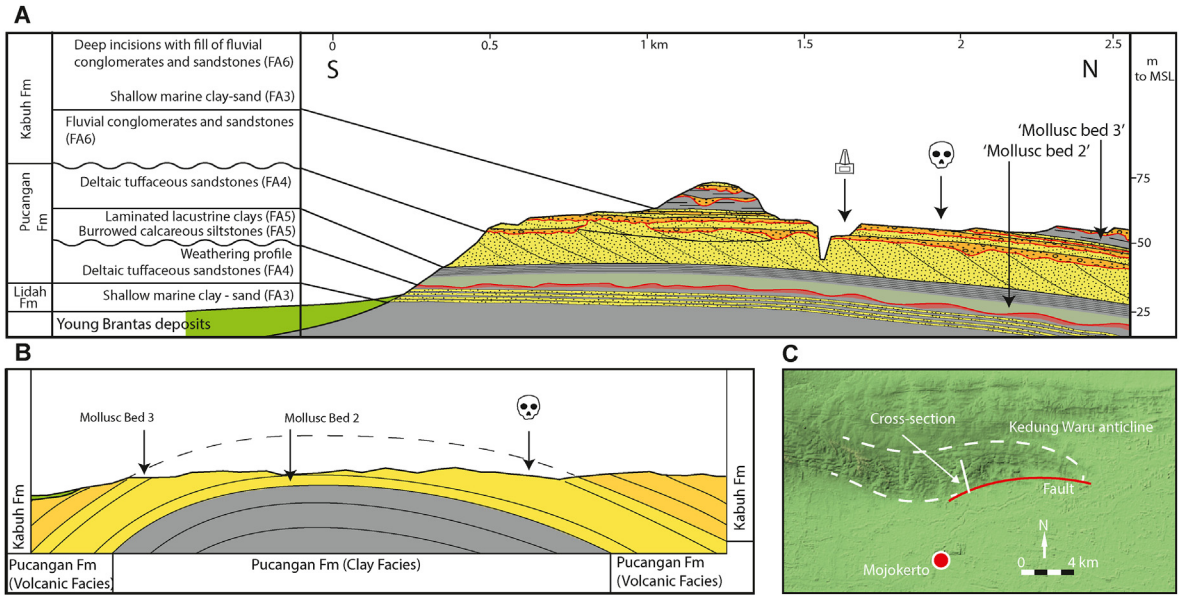

Fig. 11. A: Schematic cross-section over the Kedung Waru anticline north of Mojokerto. South flank of the anticline is missing, probably due to faulting. Fluvial strata covering the anticline erosively overlie the Early Pleistocene marine series and represent the ancient Brantas floodplain, which has been warped up and included in the fold. Cemented conglomerate lags have been prepared by erosion and form plateaus along the axis of the anticline and form cuesta-like ridges along the north flank of the anticline. B: Previous interpretation and unit definition (Duyfjes, 1936), in which the series forms an uninterrupted record. Missing south flank of the anticline was not noted. Reconstruction of historic observations is aided by the use of two prominent mollusc-bearing levels as marker beds. Mollusc bed 2 is the mollusc-bearing siltstone interval below the steeply inclined clinoforms; mollusc bed 3 is the marine interval at the top of the fluvial series. C: Location of the cross-section. Note the missing south flank of the anticline, probably by faulting.

collected from bone-bearing gravelly beds between the two mollusc beds. This suggests that the bones derive from the conglomerate lags of the three fluvial sequences that overlie the deltaic series. A monument commemorating the find of the *Homo*

erectus skullcap was placed on top of the lowest conglomerate bed, at a site north of Klagen Creek. However a later study indicated a higher conglomerate bed, exposed slightly further to the north, as the find spot (Huffman et al., 2005). Most likely, this is the conglomerate bed that forms the base of the second fluvial sequence (Fig. 10F).

6. Discussion

6.1. From back-arc basin to sheltered embayment

The calcareous and diatomaceous mudstones (FA1) that form the base of the eastern Kendeng depositional record are part of a well-studied, regional series that is recognized as the fill of the ancient back-arc basin (Lunt, 2013; Van Gorsel and Troelstra, 1981). The material dates from the Late Miocene to Pliocene and represents the final stage of the basin, in which the Miocene volcanic arc was no longer active and the influx of clastic material had largely stopped.

Planktonic foraminiferal age markers (Fig. 7) indicate that the depositional record of the Marmoyo Section dates back to the Early Pliocene. The scarce benthic foraminifera point to bathyal depth conditions**,** roughly estimated to 800 m. Moving upwards through the mudstone series of the Marmoyo Section, the introduction of benthic species such as *Bolivina robusta* points to gradual shallowing to upper bathyal depths.

The calcareous-argillaceous mudstones that form the upper part of the mudstone series reflect an increasing supply of fine terrestrial weathering products, pointing to emerging land surfaces in the vicinity. It forms the prelude of the subsequent transition to massive, plastic clays rich in fine terrestrial organic material (FA2). The geographic distribution of the clays in the subsoil of eastern Java provides an interesting insight into the depositional landscape. The material can be traced eastwards to the mostly unfolded coastal plains of Surabaya, whereas to the north and the west, the material can be traced into the Randublatung Valley (Fig. 1). Here, the clays wedge out against the southern foot slopes of the Rembang Hills and the northern foot slopes of the western Kendeng. This gives an image of a narrow, muddy marine embayment between elongate emerged ridges. We refer to this previously unrecognized Plio-Pleistocene landscape, along the western edge of the ancient Madura Strait, as the Surabaya Embayment (Fig. 12A).

There must have been a rich supply of terrestrial weathering products to the embayment, which cannot have been provided by the low-altitude ridges that formed the embayment margins, which were largely made up of calcareous strata. Sediment supply from the Sunda Shelf in north is also unlikely, as Late Pliocene carbonates below the Java Sea indicate that this area remained submerged (Lunt, 2013; Morley et al., 2016). In section 6.3 we will see that widespread emergence of this part of the Sunda Shelf occurred later, in the Early Pleistocene. But even if some areas of this carbonate platform already emerged in the Late Pliocene, they cannot have formed a significant clastic source.

A more likely source area for the clayey fill of the Surabaya Embayment is found in the west. Here, the North Serayu Mountains form an impressive mountain range, today reaching altitudes of over 2000 m + MSL. Similar to the western Kendeng, the North Serayu were formed by folding and thrusting of the fill of the Mio-Pliocene back-arc basin, during the Late Pliocene compressive stage (Satyana and Armandita, 2004). But in this area, the uplifted strata consist of turbidite claystones (Satyana, 2007), which must have made the uplift zone a massive source of easily-weatherable clastic material.

Returning to the well-dated marine series of the eastern Kendeng, we can now make an interesting reconstruction of Plio-Pleistocene landscapes in relation to tectonism and emerging surfaces. The Pliocene mudstones series was deposited in the shallowing back-arc basin, with an open connection to the Indian Ocean in the south and the submerged Sunda Shelf in the north. The increasing admixture of argillaceous material in the top of this mudstone series, which dates back to 3.8 Ma, reflects the early emergence of the North Serayu Mountains. The predominantly calcareous composition of the sediment shows that the connection with the carbonate shelf in the north was still open. The subsequent transition to plastic clays, dated to 3.0 Ma, indicates that the area became cut-off from the supply of calcareous mud, which can be explained by the emergence of the Rembang Ridge. The change in sediment composition thus signals the birth of the sheltered Surabaya Embayment (Fig. 12A).

6.2. The Pliocene regression as a function of uplift and deposition

The succession of marine mudstones and massive clays, which makes up the lower part of the Marmoyo-Sumberingin Section of Jombang up to the paleosol at 680 m, exhibits a distinctive shallowing-upward trend. A reconstruction of depositional depths (Fig. 13) indicates that the Pliocene regression was not merely an effect of sedimentary infilling of the inactive back-arc basin, but also involved uplift of around 0.5 mm/a. This uplift may have been related to isostatic rebound by the disapearance of the Miocene volcanic arc, Late Pliocene compression, or regional long-wavelength uplift.

The benthic foraminiferal assemblage of the base of the massive clays, consisting of upper bathyal species as *B. marginata* and shelf species as *A. supera* and *P. gaimardii*, suggests outer shelf depths of around 200 m. However, moving up-section through the clays, reduced occurrences of shelf species and re-appearance of bathyal species as *Uvigerina* sp., *L. pauperata* and *Gyroidina* sp. reflect deepening to upper bathyal depths, which may be roughly estimated to ~300 m, suggesting subsidence of the embayment between 3 and 2 Ma. This temporary subsidence, which also explains the great thickness of the clays, is remarkable, referring to the paleogeographic setting of an enclosed embayment surrounded by emerging ridges, under a predominantly compressive regime. Corrected for on-going sedimentation, total subsidence in this period may have amounted to ~250 m (Fig. 13). This local subsidence may have been related to complex movements along pre-existing basement faults, which are omnipresent in eastern Java, and relate to a Paleogene rift system (Husein et al., 2015). Uplift of the Rembang Hills, as well as several isolated uplift zones within the Randublatung Valley, also relate to vertical movement along basements faults.

6.3. Emergence and subsequent development of a shallow embayment

The paleosol that caps the massive clays represents emergence of the embayment floor. The clays directly below the paleosol bear no evidence of gradual shallowing, in the form of sedimentary structures or increasing occurrences of shallow-water benthic foraminifera. This suggests that emergence was caused by resumed uplift rather than by gradual depositional in-filling of the embayment (Fig. 13). Based on scarce planktonic age markers and an assumed sedimentation rate of 18 cm/ka, the age of the massive clays directly below the paleosol has been estimated to ~2 Ma (Berghuis et al., 2019). It is interesting that this age roughly corresponds with the estimated age of regional emergence of the Sunda Shelf (Lunt, 2013; Morley et al., 2016), which is generally linked to

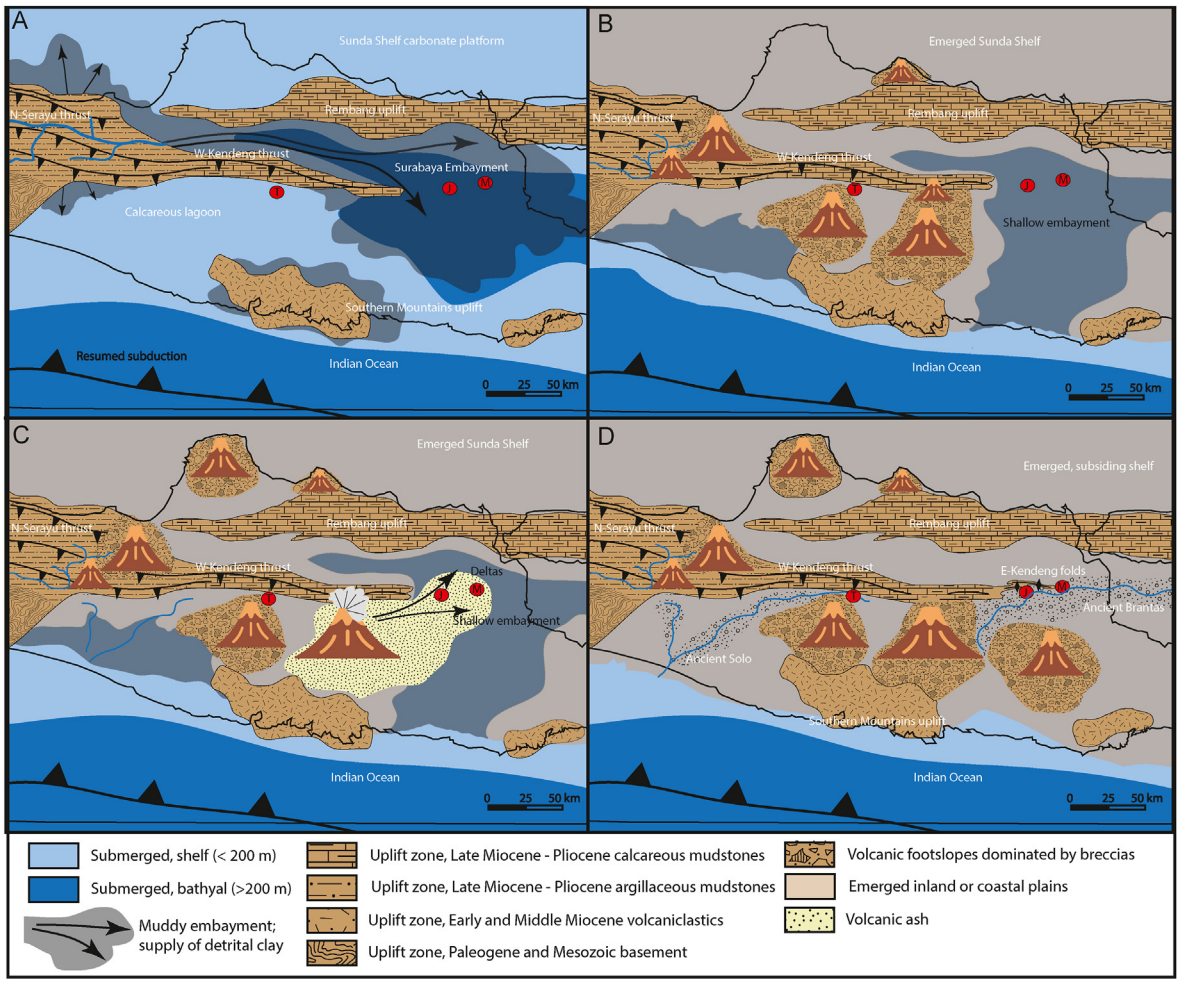

Fig. 12. Paleogeography of eastern Java, A: Late Pliocene – Early Pleistocene, ~3 Ma to 2 Ma. Narrow embayment between elongate uplift zones (Surabaya Embayment). Upper-bathyal to outer-shelf depth conditions. Sediment supply from North Serayu uplift. B: Early Pleistocene ~2 to 1 Ma. Embayment is uplifted, along with the greater Sunda Shelf region. After a stage of emergence, a shallow embayment develops. C: Early Pleistocene ~1 Ma: Explosive, high-silica eruptions of the Wilis. High supply of unconsolidated ash to the shallow embayment, development of quickly prograding deltas. D: Middle Pleistocene: Uplift and incision. Development of Brantas drainage system over the emerged shelf of the current Madura Strait.

long-wavelength uplift of the larger Sunda Shelf. This suggests that emergence of the Surabaya Embayment was, at least partly, related to regional uplift.

The estimated age of ~2 Ma for the top of the massive clays can be regarded as the maximum age of emergence of the embayment floor. The red-colored weathering profile with iron concretions testifies to a humid tropical climate, which is in line with the Early Pleistocene pollen record of eastern Java (Polhaupessy, 1990; Sémah and Sémah, 2012). Assuming a weathering rate of 1–2 cm/ka (Evans et al., 2019) and a preserved thickness of 1.5 m, the paleosol equals a minimum weathering period of 75–150 ka.

The overlying marine clay-sand alternations (FA3) reflects the development of a shallow sea. Referring to the maximum age of the paleosol and its weathering period, the maximum age of this re-submergence may be estimated to 1.9 or 1.8 Ma. Interestingly, this rough age estimate is supported by the occurrence of andesitic sand and fine gravel, at the transgression surface and in the overlying shallow marine sediment. This granular volcanic material, which is absent in the massive clays below the paleosol, indicates that re-submergence postdates the earliest Wilis eruptions of ~1.9 Ma, which are regarded as the oldest Pleistocene andesitic eruptions of this part of Java (Section 6.4).

The (temporary) re-submergence of this part of eastern Java is remarkable, as around 1.8 Ma Sundaland is generally characterized by widespread subaerial exposure. The shallow sea may have been connected to ocean waters in the east through the ancient Madura Strait (Fig. 12B), or to the Indian Ocean in the south through a tectonic gap in the Southern Mountains, forming a shallow embayment.

The preservation of ca. 125 m of sandy clays, deposited under subtidal and intertidal conditions, points to renewed, gradual subsidence (Fig. 13). The build-up of three superimposed coastal progradation sequences may relate to Early Pleistocene, low-amplitude sea-level fluctuations with a 41-ka cyclicity. Depending on the preservation of successive sea-level cycles, the shallow marine strata may cover several hundred thousand years. Unfortunately, planktonic foraminiferal age control is lost in these shallow marine strata (Section 5.1). However, an age anchor is provided the transition to the overlying deltaic series (Section 6.4).

6.4. Explosive volcanism and the development of ash-dominated deltas

The transition to clinoform-bedded tuffaceous sandstones (FA4) represents a drastic landscape change, toward a setting dominated by ash-laden rivers, supplying their sediment load to the shallow

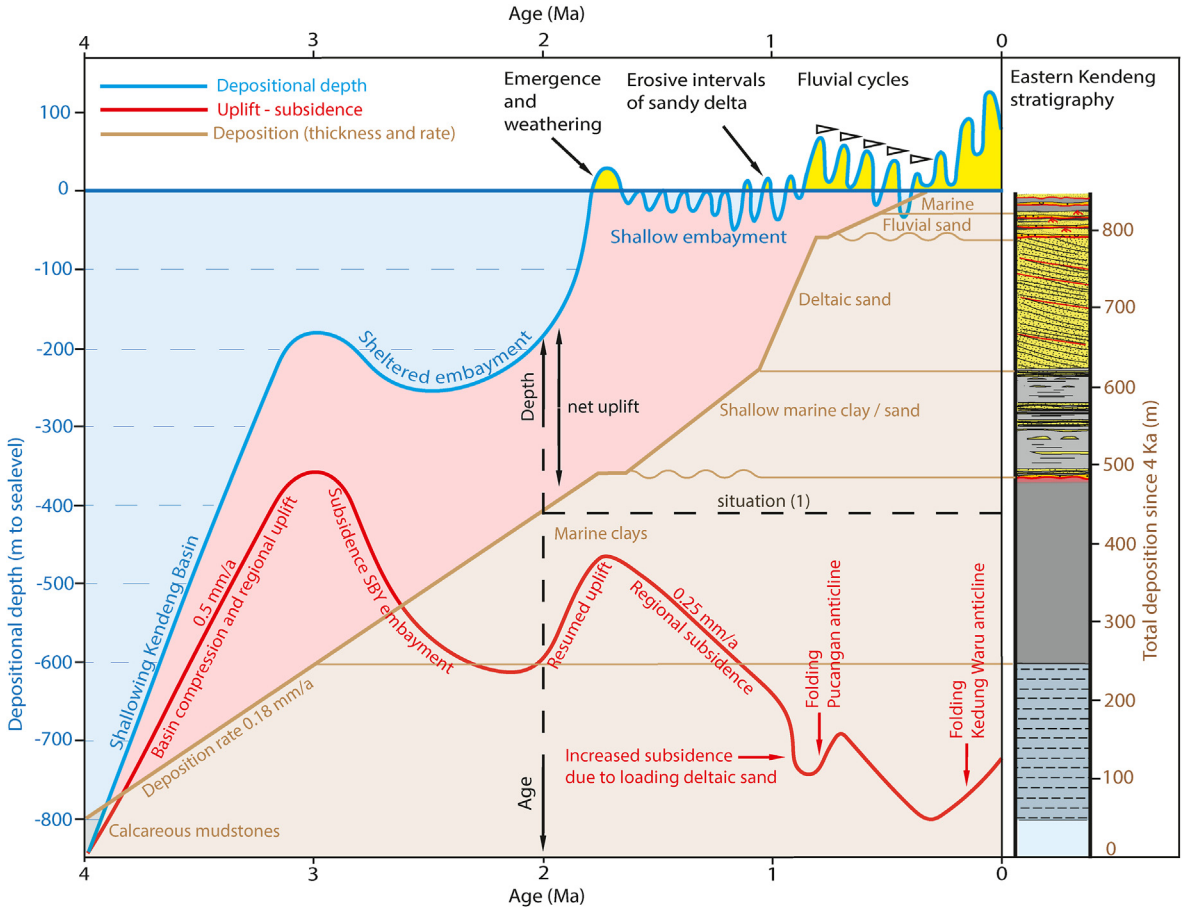

Fig. 13. Model of deposition, uplift and subsidence of the eastern Kendeng for the last 4 Ma. Depositional depth estimates have been based on benthic foraminiferal assemblages and depositional facies. Deposition rate of 0.18 mm/a has been based on planktonic foraminiferal age markers in the upper part of the calcareous mudstone series and has provisionally been extrapolated through the overlying clays. For details, see Berghuis et al. (2019). The pink area represents the difference between total deposition since T0 (4 Ma) and depositional depth, which provides insight into the vertical movement (net uplift) since T0. The red line is the resulting uplift-subsidence curve. How to read: Situation 1 (example). Age: 2 Ma; sediment: massive marine clays; deposition rate: 0.18 mm/a; depositional depth 200 m; vertical movement: uplift rate ca. 0.5 mm/a. The graph gives a general insight into the tectonic history of the eastern Kendeng. From 4 to 3 Ma the area was subject to uplift, probably representing compression of the former back-arc basin. Around 3 Ma the Surabaya Embayment developed between emerging ridges and became subject to temporary subsidence, which we relate to vertical movements along older basement faults. Uplift resumed around 2 Ma. After a stage of subaerial exposure, the area became subject to subsidence, with a rate of ~0.25 mm/a, which is within the range of regional shelf subsidence as determined by Sarr et al. (2019). Around 300 ka, the Kedung Waru fold developed, leading to local uplift. (For interpretation of the references to color in this figure legend, the reader is referred to the Web version of this article.)

embayment. This points to a stage of explosive volcanism in the hinterland, with voluminous ash falls and pyroclastic flows. The Early Pleistocene eruptive stages of the Wilis and Anjasmoro were dominated by intermediary to mafic rocks. The only recorded stage of Early Pleistocene, explosive, high-silica magmatism is associated with remnants of calderas found in the larger Wilis area. This stage is undated, but Hartono (1994) K/Ar-dated pre- and post-caldera andesite rocks, which gives a rough insight into the age the caldera stage. The early, pre-caldera eruptive stages of the Wilis are characterized by basalts, basaltic andesites and andesites with K/Ar-ages between 1.99 and 1.09 Ma. Two samples from a younger eruptive stage, post-dating the caldera, were dated to 0.81 and 0.57 Ma. Although the used bulk-dating technique is probably not very accurate, the data roughly indicate the period between 1.09 and 0.81 Ma as a time window for the caldera stage.

Assuming a causal link between this stage of explosive volcanism and the rapidly prograding deltas (Fig. 12C), the deltaic sandstones may date to ~1 Ma. Paleo-climate indicators support this age estimate: The rhythmic build-up of ashy foresets and clayey interbeds reflects episodes of peak fluvial discharge separated by longer stages of reduced discharge, which points to a strong seasonality. Eastern Java pollen records reflect a change from humid tropical conditions toward more arid conditions with a pronounced rainy season during the Mid Pleistocene Transition (Sémah et al., 2010). Moreover, Morley et al. (2020) described pollen assemblages from the deltaic beds of Mojokerto that point to a mainland vegetation dominated by grasslands.

The ash-rich deltaic series is well traceable over the folds of the eastern Kendeng and probably represents multiple, rapidly prograding deltas along a coastal plain. Seasonal discharge conditions, a thin vegetation cover and abundant fine granular volcanic material may have caused braided fluvial conditions on the plains (Ashworth et al., 1994), with frequently shifting channel patterns and river mouths.

The deltaic series gives an impression of rapid deposition and may very well cover a relatively short time period, possibly of around 100 ka. Unconformities, separating sequences of delta progradation, possibly reflect high-frequency sea-level oscillations, which may roughly be linked to lowstands in the range between MIS32 and MIS26. However, there may also be other factors involved, such as shifts of the river mouth and stages of reduced volcanic supply. A relatively short stage of deltaic progradation, and

a preserved thickness of ca. 150 m, point to considerable subsidence, which may have been partly caused by loading of the quickly accumulating sediment body and compaction of the underlying clays (Fig. 13).

6.5. The deltaic landscape of mojokerto

The bedded tuffaceous sandstones that form the base of the Mojokerto Section have relatively thick clayey interbeds and lack a prominent depositional dip, pointing to a more distal deltaic setting. The overlying rooted weathering profile reflects sea-level lowering and temporary subaerial exposure of the delta body. Organic clays with pyrite crystals, locally preserved at this level, represent coastal marsh conditions.

The overlying interval of mollusc-rich calcareous siltstones (FA5) points to re-submergence. The ash-dominated composition of the material and its position interbedded between the clinoform-bedded series, links it to the deltaic depositional landscape. We regard the sheltered, shallow marine setting as an interdistributary bay between elongate delta lobes. We infer that the volcanic ash, dominating the sediment of this facies association, was supplied to these bays during episodes of extreme run-off and flooding of the main channels on the delta plain. During subsequent, prolonged calmer stages, clear-water conditions returned and the volcanic ash became thoroughly mixed with calcareous sediment by bioturbation.

The sharp transition to laminated, lacustrine clays (FA5) points to isolation of the former bay, by delta-lobe progradation or by sea-level lowering, forming a coastal lake. The couplets of light and dark laminae probably represent seasonal variation, the lighter-colored laminae reflecting increased supply of detrital clay and fine volcanic ash during the rainy season, probably by flooding stages of the main fluvial channel. The dark laminae reflect intervening calmer periods, characterized by settling of fine organic material. The laminae may be regarded as varve couplets, representing yearly cycles of rainy and dry seasons. With an average thickness of such couplets of 3 or 4 mm, 1 m of laminated clays may represent a deposition time of ~300 years, which agrees with varve-counted sedimentation rates in similar eutrophic lakes in coastal settings (i.e. Kelsey et al., 2005). With a maximum thickness of several meters, the laminated clays represent short-lived coastal lakes.

The overlying series of tuffaceous deltaic sandstones (FA4) represents renewed delta progradation, probably caused by a shift of the river mouth. The stratigraphic position of these clinoforms suggests that the delta partly developed inside the coastal lake. This may explain the relatively steep inclination of the foresets, as freshwater conditions of the receiving basin must have caused rapid mixing and abrupt sedimentation near the river mouth, forming a Gilbert-type delta (Postma et al., 1990). The preservation of steep foresets must have been aided by the stagnant water conditions, which prevented the delta front from frequent slumping (Nemec, 1990). Moreover, the setting as a stagnant coastal lake with anoxic bottom waters explains the absence of marine fossils in the deltaic beds.

The unconformity that subdivides the inclined strata in two deltaic sets reflects a stage of subaerial exposure and the development of a grassy vegetation cover. The overlying clinoforms reflect re-submergence and continued deltaic progradation, with the flatter foresets and low quantities of admixed shell fragments pointing to a marine setting.

6.6. Fluvial incision of the delta surface

The sandy clinoforms and overlying fluvial strata have since decades been regarded as foresets and topsets (Duyfjes, 1938; Huffman and Zaim, 2003; Kumai, 1985; Morley et al., 2020). However, the clinoforms (FA4) are made up of fine-grained volcanic ash, with scarce fine pumice gravel, whereas the overlying fluvial sediment (FA6) contains polymict volcanic conglomerates rich in rounded andesite clasts. This great difference in sediment composition and texture indicates that the foresets and the overlying fluvial strata do not represent one and the same depositional system. Instead, the sharp contact between the foresets and the fluvial strata represents younger fluvial incision and forms a hiatus of unknown duration. The conglomerate bed overlying this erosive contact is a lag deposit associated with this incisive stage.

The exposures of Mojokerto provide additional evidence for this younger fluvial truncation of the deltaic series. The fluvial strata overlie the clinoforms without a trace of a sigmoidal transition. Within a deltaic setting, a sharp, planar fluvial truncation surface may be indicative of a stagnant or falling base level. However, tracing the truncation level along the Mojokerto quarries reveals an irregular erosion surface, reflecting a paleo-landscape of incised valleys, much unlike a sea-level controlled delta plain. Moreover, in areas where the delta lobes wedge out, the erosion surface continues and incises the laminated lacustrine clays, again demonstrating that fluvial truncation is unrelated to the prograding delta.

The position of the fluvial strata along the Pucangan anticline north of Jombang suggests that fluvial truncation of the deltaic sands is related to folding and uplift (Fig. 8A). The strata make up the southern footslopes of the anticline, but do not re-appear along the opposite flank. Thus far, this has been explained by lateral facies change (Fig. 8B): shallow marine clays exposed along the north flank were interpreted as the chronostratigraphic equivalent of the fluvial strata along the south flank (Duyfjes, 1938, pp. 48). This stratigraphic approach is based on the assumption that (1) we are looking at an uninterrupted series and (2) folding postdates deposition of the entire series. However, the erosive base of the fluvial strata shows that the assumption of uninterrupted sedimentation is incorrect. The occurrence of the fluvial strata along the south flank of the anticline indicates that the material was deposited alongside the emerging fold, which suggests that the incisive lower boundary of the strata is linked to fold-related uplift. Differences in tectonic dip support this landscape model. The deltaic sandstones underlying the fluvial strata have an average southward tectonic dip of 30°, whereas the fluvial strata dip only 10°–15°, suggesting that fluvial deposition postdates initial folding and uplift of the anticline. We conclude that the fluvial strata are part of a fluvial fill that formed in the lowlands south of the upcoming anticline (Fig. 12D) and that the erosive base reflects fold-related uplift. The current position of the fluvial strata, uplifted and slightly tilted along the southern foot slopes of the Pucangan anticline, must be a result of later or continued folding.

In the Kedung Waru anticline of Mojokerto, we find the same fluvial series, but here it is included in the fold (Fig. 11A). This illustrates the younger age of the anticline, which is also apparent from its gently dipping flanks and lower altitude. The fluvial strata have a similar incisive lower boundary over the underlying deltaic strata as in the Jombang area, but at this site without a noticeable angular disconformity, as incision predates folding. It is tempting to regard the incision surfaces over the deltaic series of Jombang and Mojokerto as isochronous. Possibly, folding of the Pucangan anticline was accompanied by uplift of a wider area, causing fluvial incision around Jombang and Mojokerto. However, the erosion surface may just as well have a more complex background, reflecting advancing uplift and sea-level cycles.

6.7. Aggradation and degradation of the Middle Pleistocene Brantas

The fluvial series of Jombang and Mojokerto marks the

development of a drainage system with its headwaters in the volcanic highland of Mounts Wilis and Anjasmoro and with wide floodplains south of the upcoming eastern Kendeng anticlines (Fig. 12D). This fluvial system was highly similar to the current Brantas and can be regarded as the river's earliest stage.

On seismic profiles of the Madura Strait, the Middle Pleistocene fluvial system can be traced eastwards toward the shelf edge, suggesting a position of Mojokerto ~200 km inland from the coastline (Susilohadi, 1995). The seismic profiles show a prominent erosive surface over the Pliocene marine substrate, testifying to prolonged Madura Strait exposure. This basal erosion surface is currently found ca. 200 m below sea level and is covered with ~150 m of marine sediment, consisting of several sequences, each with an incisive base, reflecting intermittent submergence and drainage of the shelf (Fig. 14A). A similar build-up of the seabed has been reported from seismic profiles of the Java Sea (Darmadi et al., 2007). Sarr et al. (2019) and (Husson et al., 2020) linked this to regional, long-wavelength subsidence of the shelf, with the marine sequences overlying the basal unconformity representing an intermittent regime of transgressions dating back to MIS11.

A graphical representation of the subsiding Madura Strait shelf, against the background of the Pleistocene sea-level curve (Bintanja and van de Wal, 2008), provides insight into this process of progressive submergence (Fig. 14C). The black line represents the subsiding shelf edge (current depth 175–200 m) under a regional shelf subsidence rate of 0.2 mm/ka (Sarr et al., 2019). This indicates that the subaerially exposed Madura Strait area may have experienced minor overflows of the shelf edge during the highstands of MIS15 and MIS13, but only from MIS11 onwards it fully submerged during highstand conditions.

This landscape model of a gradually subsiding shelf provides a mechanism to explain the aggradation-degradation cycles as recorded by the Mojokerto fluvial series. The cyclic build-up of the fluvial series probably has a complex background, related to sea-level fluctuations, tectonism, climate change and varying volcanic supply. However, Veldkamp and Tebbens (2001) indicated that in the subsiding lower reaches of large Pleistocene rivers, sea-level fluctuations are often the dominant mechanism controlling aggradation and degradation cycles, filtering out the impact of other factors controlling river behavior. We therefore provisionally regard the fluvial cycles of the Mojokerto record as responses to intermittent, sea-level controlled drowning of the floodplain downstream of Mojokerto.

For a reconstruction of aggradation-degradation cycles, we simulated the equilibrium profile of the Middle Pleistocene Brantas, referring to the similarly dimensioned and well-studied

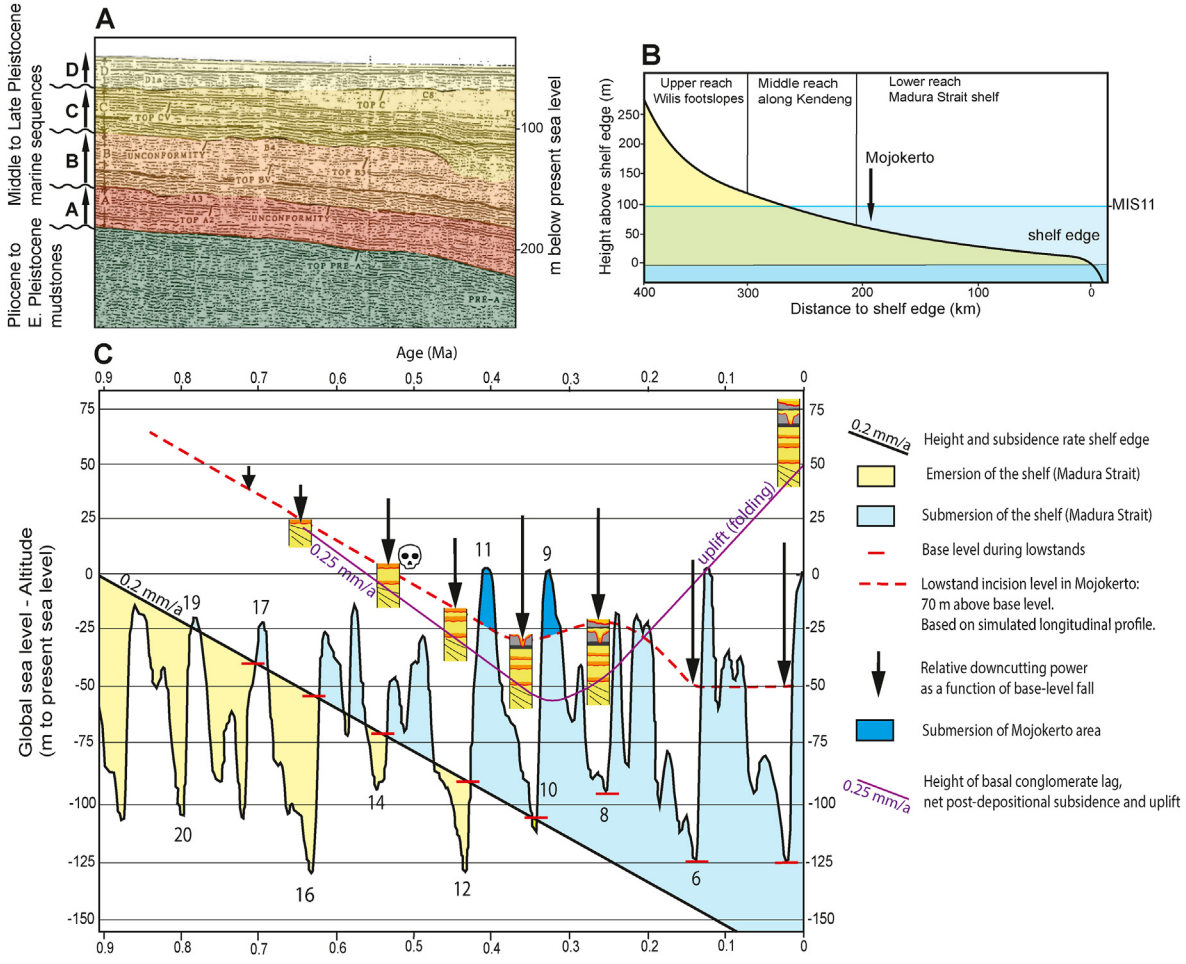

Fig. 14. ASeismic profile over the Madura Strait (Susilohadi, 1995). Basal unconformity represents prolonged Early Pleistocene subaerial exposure. Overlying marine sequences with incised top represent intermittent re-submergence of the shelf during highstands, under regional subsidence. First large-scale submergence is linked to MIS 11 (Sarr et al., 2019). 14B: Simulated longitudinal equilibrium profile of the Middle Pleistocene Brantas during sea-level lowstand, with water level below the shelf edge. Subsidence resulted in overflows of the shelf edge during highstands, reaching increasingly further inland. During MIS11, flooding of the Brantas drainage system reached beyond Mojokerto. 14C: Reconstruction of successive fluvial cycles in relation to sea-level fluctuations and subsidence. The Perning skullcap was found in the conglomerate lag that forms the base of the second fluvial sequence, suggesting an MIS14 age. Sea-level curve based on Bintanja and van de Wal, 2008.

longitudinal profile of the Meuse (Tebbens et al., 1999). Like the ancient Brantas, this river has a ca. 200 km long lower reach of coastal lowlands, and a slightly uplifted middle reach. Middle Pleistocene Mojokerto was part of the subsiding lower reach of the river, with a setting similar to the present-day coastal plains of Surabaya and Mojokerto. Referring to the gravelly texture of the channel deposits and a position adjacent to the Kendeng uplift, we projected the position of Middle Pleistocene Mojokerto close to the hinge line that marks the transition toward the uplifted middle reach, with an estimated riverbed height of ~70 m above base level in equilibrium conditions (Fig. 14B).

Our reconstructions suggest that before MIS19, sea level probably remained below the edge of the subsiding shelf and sea-level fluctuations did not have a notable impact on river behaviour. The MIS19 and MIS17 highstands may have caused minor flooding of the river-mouth area, but we assume that the Brantas profile remained in its equilibrium state, with around Mojokerto a stable altitude of ~70 m above the shelf edge (Fig. 14B). MIS15 caused the first stage of more significant flooding of the shelf edge, forcing the river to readjust its longitudinal profile by gradient backfilling in its downstream reach. We provisionally regard the first aggradational fluvial sequence of Mojokerto, overlying the basal conglomerate bed, as this MIS15-related fluvial depositional wedge.

The overlying erosion surface, marked by the second conglomerate lag, is tied to the MIS14 lowstand. Likewise, the subsequent aggradational sequence and the overlying incisive conglomerate bed may be tied to MIS13 and MIS12. During the two intervening lowstands (MIS14 and MIS12), sea levels dropped below the shelf edge and the river may have degraded its valley back to its equilibrium state 70 m above the shelf edge. The fact that around Mojokerto, fluvial aggradation sequences are partly preserved suggests that valley-degradation stages were not long or intense enough to re-establish the river's equilibrium profile. But the partial preservation of aggradation sequences may also have had other causes, such as a local subsidence rate that slightly exceeded regional subsidence. In Fig. 14B, we projected the base of each consecutive incision stage at the assumed equilibrium position of 70 m above base level, which results in an (apparent) local subsidence rate of 0.25 mm/a.

MIS11 is characterized by an extreme sea-level rise, reaching a level that slightly exceeds present-day sea level. In combination with continued shelf subsidence, this resulted in widespread submergence of the shelf. Our river profile reconstructions suggest that the Brantas valley drowned beyond Mojokerto, setting the floodplain of Mojokerto ca. 25 m below sea level. This would explain the build-up of the third aggradational sequence of Mojokerto, which grades upwards into this first marine interval. The subsequent MIS10 lowstand resulted in a rapid base-level fall of more than 100 m. We relate the deep, channelled incisions into the marine interval of Mojokerto to this stage of intense fluvial downcutting. During the subsequent highstand of MIS9, this incised landscape again drowned, forming the second marine interval, which again became incised during the subsequent lowstand of MIS8.

From MIS8 onwards, lowstand sea levels remained above the shelf edge and consequently the Brantas base level was determined solely by global sea level. Assuming that MIS8 degradation reached the river's equilibrium profile, with a local erosion base 70 m above lowstand sea level, suggests a change in local tectonic conditions toward uplift (Fig. 14B). This is not surprising, as currently the fluvial series forms the top of the Kedung Waru anticline. Apparently, Kedung Waru folding dates back to ca. 300 ka, pushing up the valley floor and forming an anticline alongside the Brantas. Younger sea-level cycles must have continued to cause valley degradation and aggradation, but only in the active floodplain south of the anticline. The MIS6 and MIS4 degradation stages must have incised the valley floor down to ~50 m below present-day sea level. The gravelly lags of these incision stages are buried under the Holocene fill that constitutes the current Brantas floodplain.

6.8. Age of the fossil-bearing fluvial strata of mojokerto

Our study suggests that the bone-bearing fluvial strata of Mojokerto are significantly younger than previously thought. Whereas commonly regarded as Early Pleistocene, we propose a Middle Pleistocene age, roughly ranging between MIS16 and MIS11. This new age estimate solves an important biostratigraphic inconsistency, as the vertebrate fossil assemblage of Mojokerto is commonly recognized as the Middle Pleistocene Kedung Brubus Fauna. Moreover, it is in line with the climate record of eastern Java. Several authors reported humid tropical conditions during most of the Early Pleistocene, changing toward more arid conditions with a pronounced rainy season during the Mid Pleistocene Transition, referring to pollen records (Sémah et al., 2010), paleosols (Berghuis et al., 2021; Brasseur et al., 2011) and isotope ratios in herbivore molars (Janssen et al., 2016; Puspaningrum et al., 2020). The previous, Early Pleistocene age estimates of the fluvial, fossil-bearing strata therefore imply that they were formed under humid tropical conditions, however floodplain soils with carbonate concretions and grassy rootlets, as well as a grass-dominated pollen record, point to a relatively dry climate and open vegetation.

However, a Middle Pleistocene age is in conflict with the published paleomagnetic measurements of Mojokerto (Hyodo et al., 1993). Our new age model suggests that the transition from predominantly reversed polarities in the deltaic beds to predominantly normal or intermediate polarities in the overlying fluvial beds represents the Brunhes-Matuyama polarity change, however this is incompatible with the reported reversed polarities higher in the stratigraphy. Magnetic overprint of the primary signal cannot explain this discrepancy, as after the Brunhes-Matuyama transition, no significant polarity changes have occurred. The discrepancy may be related to Middle Pleistocene geomagnetic excursions (Laj and Channell, 2007) or to different stratigraphic interpretations. With respect to the latter, we note that Hyodo et al. (1993) described a 200 m thick depositional record along Kepuhklagen Road, with long unexposed intervals and undetailed facies descriptions, based on earlier work of Kumai (1985). Sampling was carried out along the roadside section over a distance of more than 2 km, extrapolating the sample positions to their 200 m long stratigraphic column. Our stratigraphic section (Fig. 9), based on carefully measured quarry sections directly east of the road, covers a total exposed thickness of only 53 m, leaving virtually no unexposed intervals. Kumai (1985) and Hyodo et al. (1993) based their stratigraphic interpretations on Duyfjes' (1938) cross-section over the area, which is, as we showed in section 5.2 and Fig. 11, an incorrect representation of the Kedung Waru fold.

Our revised age estimate for the fluvial strata of Mojokerto also conflicts with the published radiometric ages of 1.81 ± 0.04 Ma (Swisher et al., 1994) and 1.49 ± 0.13 Ma (Morwood et al., 2003). These ages, either crystallization or eruption ages, have been accepted to approximate the age of deposition, based on the assumption that pumice-bearing conglomerate beds represent 'short influxes of coarse volcanic material to the delta plain, triggered by distant volcanism' (Huffman, 2001; Huffman and Zaim, 2003). For the conglomerate beds this is highly unlikely, considering the vast surface of the floodplain and the great distance to the volcanoes. Moreover, it is in contradiction with the polymict composition and moderate to well rounding of the material, and with the incisive base of the beds. These conglomerate beds are clearly lags associated with fluvial incision stages and are made up of reworked material, which readily explains the old radiometric

ages. Morwood et al. (2003) reportedly sampled the dated pumice from a 15 cm thick interbed dominated by pumice gravel, which the authors relate to contemporary eruptions. This may indeed be a valid argumentation. But on the other hand, pumice gravel is one of the most common components of the polymict conglomerates. Local and hinterland incision must therefore have involved remobilization of older, loose pumice, which may occasionally have become concentrated in fluvial sediment by selective sorting.

6.9. Age and habitat of the mojokerto Homo erectus

Our reconstructions of fluvial incision and aggradation cycles indicate that the conglomerate bed that yielded the Mojokerto skullcap may be linked to the MIS14 lowstand, which dates to ~550 ka (Railsback et al., 2015). The vertebrate fossils in the incisive conglomerate beds were found as single bones and bone fragments. Locally, these conglomerates are particularly rich in fossils, pointing to hydraulic accumulation, possibly in the inside bend of the meandering channel. The bones may represent a contemporaneous fauna, deriving from carcasses on the floodplain, which were picked up during flooding stages and re-deposited in the channel. However, considering the incisive background of the conglomerate beds, bones may also have been reworked from underlying aggradational fluvial sequences. Fluvial incision may have preferentially removed fine sediment, leaving a lag of skeletal material, exhumed from the previous fluvial sequence (Rogers, 2007). This implies that the hominin skullcap may either be contemporaneous with the MIS14 conglomerate bed in which the fossil was found, or may have been reworked from the underlying MIS15 aggradational sequence, implying a possible age range of ~600–550 ka. It cannot be ruled out that the fossil was reworked from even older strata, eroded upstream. However, referring to the fragile nature of the skullcap and the absence of abrasion marks, such a background is considered unlikely.

Our re-interpretations also imply a revision of the habitat of the Mojokerto *Homo erectus*. Previously regarded as a coastal environment, based on an assumed topset relation with the underlying deltaic series (Huffman, 2001; Huffman and Zaim, 2003; Morley et al., 2020), we replace this image for the inland floodplain of the ancient Brantas. Floodplain soils with carbonate concretions and grassy rootlets point to a relatively dry climate and open vegetation. A published record of pollen and spores from the fluvial series of Mojokerto reflects a vegetation dominated by grasses with few trees, with local swamp forests dominated by marsh ferns (Morley et al., 2020). The swamp forests are probably related to the low-lying, frequently inundated floodplains of the anastomosed river. Mangrove pollen are scarce or absent in the fluvial series, confirming a setting that was, at least most of the time, at considerable distance from the coast. Scattered mangrove pollen were found shortly below the hominin bed, pointing to an approaching coastline at the top of the underlying fluvial sequence. The hominin-bearing conglomerate bed, probably representing a subsequent lowstand, is devoid of mangrove pollen. Scattered mangrove pollen were also reported higher-up in the fluvial series, below the marine interval, again heralding the approaching coastline. Scarce occurrences of pollen from montane trees must have been transported from the forested slopes of Mounts Wilis and Anjasmoro.

Although climate conditions may have been dryer than today, the large and forested hinterland probably secured perennial discharge of the river. This year-round availability of water, and the presence of herds of grazers, which dominate the local vertebrate-fossil assemblage, must have made the Middle Pleistocene Brantas valley and the surrounding grass-covered plains a suitable area for enduring hominin presence.

6.10. Validating the revised age model of the mojokerto fossiliferous beds

To test our age estimate for the fossiliferous fluvial deposits, single-grain Ar/Ar dating may be carried out on multiple volcanic hornblende and potassium feldspar crystals, following the approach of Hilgen, (under review). In order to get insight into a possible difference between hornblende crystallization ages and eruption ages, additional fission-track dating may be carried out, preferably on minerals from the same pumice as sampled for the Ar/Ar dating. We postulate that this will yield a wide range of ages, representing the complex incisive origin of the sediment. The age range will provide insight into the maximum age of a layer, with the youngest age of the range ideally being a maximum age close to the depositional age. Our age framework suggests that the fluvial sequences at the top of the Mojokerto series, overlying the first marine incursion, relate to stages of rising sea level after the lowstands of MIS10 and MIS8 (Fig. 14). This implies that ages may fall within the range of optical dating methods, which can be tested by OSL-dating.

The fossiliferous strata of Mojokerto consist of superimposed fluvial sequences separated by erosion surfaces. This asks for a sampling and dating strategy that aims for dating individual sequences. The numerical ages can then be used to validate or adjust our correlations with the Pleistocene sea-level curve.

Renewed paleomagnetic measurements, in combination with multiple Ar/Ar dating, will also be of great value. Sampling can be carried out in open quarry sections, to make sure that there is no uncertainty over stratigraphic position. And again, sampling and interpretation should bear in mind the build-up of stacked depositional sequences.

A significant age difference is expected between the sediment on either side of the basal fluvial erosion surface, i.e. between the top of the deltaic series and the lowest fluvial sequence. As we relate the stage of delta progradation to explosive volcanism, this sediment may offer good possibilities to find contemporaneous eruption products, providing an important age constraint for the overlying fluvial strata that likely have a more mixed composition.

6.11. Implications for the eastern java stratigraphy

Our re-interpretation of the eastern Kendeng reference sections sheds a new light over the significance of Duyfjes' (1938) stratigraphy. We identified most of the sedimentary record as the fill of a local embayment. Extrapolation of these units to areas such as Trinil, located outside this former embayment, has little lithological or paleo-environmental significance and merely suggests age relations, most of which are unproven. The only exception is the Kalibeng Formation, which is a regional unit that predates the embayment.

Duyfjes indicated the marine clays, overlying the Kalibeng Formation, as the Clay Facies of the Pucangan Formation. The clays represent the most prominent facies of the embayment fill and are also found in the subsoil of the Randublatung Valley and around Surabaya. The eastern Kendeng Hills are in fact a series of young folds over the former embayment area, offering a unique insight into the embayment fill. Unfortunately, early researchers describing wells in the adjacent plains were not fully aware of this situation and gave these clays different names, such as Mergel Ton (Trooster, 1937), Blue Clays (van Bemmelen, 1949) or Lidah Formation (Brouwer, 1966). Lately, there is a tendency to expand the name Lidah Formation to the clays exposed in the eastern Kendeng (Pringgoprawiro, 1983), which is a stratigraphic improvement that we follow in this paper.

We found the clays of the eastern Kendeng to be made up of two

series, separated by a paleosol. The lower series, consisting of massive clays with a shelfal and upper bathyal benthic foraminiferal fauna (FA2), represents the early, deep-water stage of the Surabaya Embayment. The overlying series consist of shallow marine clay-sand alternations with a neritic benthic foraminiferal fauna and shell fragments (FA3) and represent a later marine incursion, in the form of a shallow embayment. We propose to assign these series to separate members, Lidah-1 and Lidah-2. Wells in the nearby plains (Bolli, 1966) indicate a similar build-up, of massive clays that may be referred to as Lidah-1 overlain by sandy clays that may be referred to as Lidah-2. However, we note that the chronological and paleogeographic significance of the two clay series may differ from site to site and needs further investigation. For example, in the coastal plains, the top of the clays is probably of Middle Pleistocene age, representing intermittent transgressions dating back to MIS11.

In the eastern Kendeng, the shallow marine clays are capped with tuffaceous deltaic sands (FA4), which we linked to a short stage of explosive volcanism. Similar strata have not been reported from wells in the nearby Randublatung Valley, suggesting that the material wedges out to the north and east, or that the shallow marine inlet that was filled by the delta did not cover the entire area of the previous deep-water embayment (Fig. 12C). Duyfjes regarded this material as the Volcanic Facies of the Pucangan Formation. We propose to hold on to this well-known unit name, but restrict its use to the tuffaceous deltaic series of the eastern Kendeng. Extrapolations to other areas and to strata with different facies suggest unfounded age relations and should be avoided.

The fluvial top of the eastern Kendeng series (FA6) is not part of the actual embayment fill, but relates to the Brantas drainage system that developed later. This readily explains the problems involved with the historic correlations, for example to the Trinil area (Fig. 2). Although ages may partly overlap, the fluvial strata of the eastern Kendeng and Trinil represent different drainage systems, with other source areas of their sediment load and a different tectonic and volcanic control of incision and aggradation. The fluvial strata of the ancient Brantas system may be referred to as the Kabuh Formation, holding on to Duyfjes' unit name. Note that Duyfjes placed the lower boundary of the Kabuh Formation ca. 20 m higher, adding the base of the fluvial strata to the Pucangan Formation, based on an assumed difference in vertebrate fossil assemblages within the fluvial series. After the faunal revision by De Vos and Sartono (1982), this practice has lost its significance. We propose to place the boundary between the Pucangan and Kabuh Formations at the erosive base of the fluvial series.

7. Conclusions

The regressive series of the eastern Kendeng represents the fill of a relatively deep Plio-Pleistocene embayment, situated between emerging uplift zones, which we refer to as the Surabaya Embayment. The eastern Kendeng stratigraphic units, defined in the 1930's and until today regarded as a regional standard, have local significance only.

The embayment formed ~3 Ma, as the emerging Rembang Ridge shut-off the area from the calcareous shelf in the north. Around 2 Ma the embayment emerged, along with the greater Sunda Shelf, which left a paleosol on the >200 m thick clayey embayment fill. Shallow marine clays overlying the paleosol reflect renewed submergence and the development of a shallow embayment.

A transition to deltaic sandstones indicates a sharply increased supply of volcanic ash, which we relate to a stage of explosive, high-silica volcanism of the Wilis and which probably dates from the period between ~1.09 and 0.81 Ma. The Mojokerto delta, with its steeply inclined foresets, was part of this larger delta landscape and formed in an interdistributary bay and associated coastal lake.

The top of the eastern Kendeng series consists of fluvial strata, which have an incisive base and are unrelated to the underlying deltaic deposits. We link this fluvial cover to the early Brantas, which had a similar position as the present-day Brantas, but continued over the emerged Madura Strait toward the shelf edge, ~200 km to the east. Shelf subsidence in combination with sea-level fluctuations caused intermittent flooding of the shelf edge.

The fluvial, vertebrate-bearing strata have a cyclic build-up, representing alternating aggradation and degradation stages, which we provisionally link to sea-level fluctuations. Our reconstruction of these aggradation and degradation stages provides a new age framework. Previously regarded as Early Pleistocene, we propose a Middle Pleistocene age for the fluvial strata. This solves an important biostratigraphic inconsistency, as the vertebrate fossil assemblage of the material is commonly recognized as the Middle Pleistocene Kedung Brubus Fauna.

We link the conglomerate bed that yielded the Mojokerto skullcap to lowstand MIS14, with an age of ~550 ka. The fossil may be contemporaneous to this conglomerate bed, but considering the incisive background of the bed, it may also have been reworked from the previous aggradational sequence linked to MIS15, dating to ~600 ka.

Our age estimate of the hominin-bearing conglomerate bed of Mojokerto is significantly younger than the published Ar/Ar-age of 1.81 ± 0.04 Ma (Swisher et al., 1994) and fission track-age of 1.49 ± 0.13 Ma (Morwood et al., 2003). These authors linked the conglomerates to volcanic events, assuming that the obtained numerical ages approximate the age of deposition. However, our re-interpretation of the conglomerate beds as fluvial lags associated with incisive stages of the Brantas, implies that the material probably derived from an incised volcanic hinterland. To test our age estimates, a combination of multiple single-grain Ar/Ar and fission-track dating may be carried out. We expect that this will yield a wide range of ages, with the youngest age of the range ideally being a maximum age close to the depositional age. The youngest strata of the fluvial series may fall into the age range for OSL-dating.

A Middle Pleistocene age of the fossiliferous strata of Mojokerto is supported by normal paleomagnetic polarities. However, Hyodo et al. (1993) reported a return to reversed polarities higher in the stratigraphy, which conflicts with our age interpretation. We infer that this discrepancy is related to a Middle Pleistocene magnetic excursion or to the previous, incorrect interpretation of the local stratigraphy, which was based on roadside observations with thick unexposed intervals. Our interpretations have been based on a study of recent sand quarries, which provide a full exposure of the strata that make up the anticline. A renewed paleomagnetic study, based on samples from open quarry sections, may provide a final answer on this matter.

Finally, our re-interpretations involve a revision of the habitat of the Mojokerto *Homo erectus*. The previous claims of a coastal habitat were based on an assumed foreset-topset-relation with the underlying deltaic series. We replace this for the inland fluvial plains of the perennial Brantas, surrounded by savannah-like plains.

Author contribution

HB, AV, and JJ designed the study. JJ and SA initiated the overarching research project and together with SN and IK ensured embedding within the Indonesian research infrastructure. HB directed the field study and analysis of the stratigraphic data, and wrote the manuscript. AV, SA, SH, EP, TvK and JJ participated in the field study and analysis of the data. EP made and interpreted the

Digital Elevation Models. SN, RAD and UPW analysed the consequences of the study for the prevailing frameworks for vertebrate biostratigraphy and hominin settlement on Java. ST analysed and interpreted foraminiferal data and deep marine environments. JJ and SA are the Principal Investigators of the research project. All authors contributed to writing, reviewing and final approval of the manuscript.

Declaration of competing interest

The authors declare that they have no known competing financial interests or personal relationships that could have appeared to influence the work reported in this paper.

Data availability

Data will be made available on request.

9. Acknowledgements

This study was carried out with permission of the Indonesian Ministry of Research, Technology and Higher Education (RISTEK research permits: 263/SIP/FRP/ES/Dit. KI/VII/2016 of Josephine Joordens; 284/SIP/FRP/E5/Dit.KI/IX/2018 and 343/E5/E5.4/SIP/2019 of Harold Berghuis) under the project 'Studying Human Origin in East Java'. We thank Arkenas and in particular Dr. I Made Geria for facilitating our inspiring and enduring cooperation. We are grateful to the pak Parman and the other people of Marmoyo, Sumberingin, Kabuh and Perning for their hospitality and support. We thank Frank Wesselingh and Bert Hoeksema for their mollusc and coral identifications. The fieldwork was funded by the Treub Foundation (Maatschappij voor Wetenschappelijk Onderzoek in de Tropen), the Faculty of Archaeology, Leiden University and the Dutch Research Council NWO (Grant number 016. Vidi.171.049).

Appendix A. Supplementary data

Supplementary data to this article can be found online at https://doi.org/10.1016/j.quascirev.2022.107692.

References

Alqahtani, F.A., Johnson, H.D., Jackson, C.A.-L., Som, M.R.B., 2015. Nature, origin and evolution of a late Pleistocene incised valley-fill, Sunda shelf, southeast asia. Sedimentology 62, 1198–1232.

Ashworth, P.J., Best, J.L., Leddy, J.O., 1994. The physical modelling of braided rivers and deposition of fine-grained sediment. In: Process Models and Theoretical Geomorphology§. Wiley and sons, Chichester, pp. 115–139.

Berghuis, H.W.K., Troelstra, S.R., Zaim, Y., 2019. Plio-pleistocene foraminiferal biostratigraphy of the eastern Kendeng zone (Java, Indonesia): the Marmoyo and Sumberingin sections. Palaeogeogr. Palaeoclimatol. Palaeoecol. 528, 218–231. https://doi.org/10.1016/j.palaeo.2019.05.008.

Berghuis, H.W.K., Veldkamp, A., Adhityatama, S., Hilgen, S.L., Sutisna, I., Barianto, D.H., Pop, E.A., Reimann, T., Yurnaldi, D., Ekowati, D.R., 2021. Hominin homelands of east Java: revised stratigraphy and landscape reconstructions for plio-pleistocene Trinil. Quat. Sci. Rev. 260, 106912.

Bhattacharya, J.P., 2006. Deltas.

Bintanja, R., van de Wal, R.S.W., 2008. North American ice-sheet dynamics and the onset of 100,000-year glacial cycles. Nature 454, 869–872. https://doi.org/10.1038/nature07158.

Blow, W.H., 1969. Late middle eocene to recent planktonic foraminiferal biostratigraphy. In: Proceedings of the First International Conference on Planktonic Microfossils. EJ Brill, Leiden, pp. 199–422.

Bolli, H.M.…, , 1966. The Planktonic Foraminifera in Well Bodjonegoro-1 of Java. Geologisches Institut der Eidg. Technischen Hochschule und der Universität.

Bolli, H.M., Saunders, J.B., Perch-Nielsen, K., 1989. Plankton Stratigraphy: Volume 1, Planktic Foraminifera, Calcareous Nannofossils and Calpionellids. CUP Archive.

Brasseur, B., Sémah, F., Sémah, A.-M., Djubiantono, T., 2011. Approche paléopédologique de l'environnement des hominidés fossiles du dôme de Sangiran (Java central, Indonésie). Quaternaire 22, 13–34.

Brouwer, J., 1966. Stratigraphy of the Younger Tertiary in North-East Java and Madura. Bataafse Internationale Petroleum Maatschappij.

Cosijn, J., 1932. Tweede mededeeling over het voorkomen van fossiele beenderen in het heuvelland ten Noorden van Djetis en Perning (Java). Geol. Mijnbouwk. Gen. en Kol., Geol. 135–148.

Cosijn, J., 1931. Voorlopige mededeeling omtrent het voorkomen van fossiele beenderen in het heuvelterrein ten Noorden van Djetis en Perning. Verh. Geol. Mijnbouwk. Gen. en Kol., Geol. 113–119.

Darmadi, Y., Willis, B.J., Dorobek, S.L., 2007. Three-dimensional seismic architecture of fluvial sequences on the low-gradient Sunda Shelf, offshore Indonesia. J. Sediment. Res. 77, 225–238.

De Vos, J., Sartono, Hardja-Sasmita, 1982. The fauna from Trinil, type locality of Homo erectus: a reinterpretation. Geol. Mijnbouw 61, 207–211.

De Vos, J., Sondaar, P., 1994. Dating hominid sites in Indonesia. Science 266, 1726–1727.

Dennell, R., 2009. The Palaeolithic Settlement of Asia. Cambridge University Press.

Dubois, 1907. Eenige van Nederlandschen kant verkregen uitkomsten met betrekking tot de kennis der Kendeng-fauna (fauna van Trinil). Tijdschrift van het Koninklijk Nederlandsch Aardrijkskundig Genootschap 449–458.

Dubois, 1894. Pithecanthropus erectus: eine menschenaehnliche Uebergangsform aus Java. Landesdruckerei.

Duyfjes, J., 1938. Toelichting Bij Blad 110 (Modjokerto), Geologische Kaart Van Java Schaal 1: 100.000. Bandung. Dienst van den Mijnbouw in Nederlandsch-Indie.

Duyfjes, J., 1936. Zur Geologie und Stratigraphie des Kendenggebietes zwischen Trinil und Soerabaja (Java). De Ingenieur ned-Indie 4, 136–149.

Elliott, T., 1986. Siliciclastic shorelines. Sedimentary environments and facies, 615–155.

Evans, D.L., Quinton, J.N., Tye, A.M., Rodés, Á., Davies, J.A.C., Mudd, S.M., Quine, T.A., 2019. Arable soil formation and erosion: a hillslope-based cosmogenic nuclide study in the United Kingdom. SOIL 5, 253–263.

Genevraye, P.D., Samuel, L., 1972. Geology of the Kendeng zone (central & east Java). Indonesian petroleum association. Annual Convention Proceedings 1, 17–30.

Hall, R., Spakman, W., 2015. Mantle structure and tectonic history of SE Asia. Tectonophysics 658, 14–45.

Hamilton, W.B., Pertambangan, I.D., Development, U.S.A. for I., 1979. Tectonics of the Indonesian Region. U.S. Govt. Print. Off.

Hartono, U., 1994. The Petrology and Geochemistry of the Wilis and Lawu Volcanoes, East Java, Indonesia (Phd). University of Tasmania.

Hilgen et al., under review. The stratigraphy and age of the classic Homo erectus-bearing succession at Trinil (Java, Indonesia). Journal of Human Evolution..

Huffman, O.F., 2001. Geologic context and age of the perning/mojokerto Homo erectus, east Java. J. Hum. Evol. 40, 353–362. https://doi.org/10.1006/jhev.2001.0464.

Huffman, O.F., Shipman, P., Hertler, C., de Vos, J., Aziz, F., 2005. Historical evidence of the 1936 Mojokerto skull discovery, east Java. J. Hum. Evol. 48, 321–363. https://doi.org/10.1016/j.jhevol.2004.09.001.

Huffman, O.F., Zaim, Y., 2003. Mojokerto Delta, East Jawa; paleoenvironment of Homo modjokertensis–first results. Journal of Mineral Technology 10, 53–82.

Husein, S., Kakda, K., Aditya, H.F.N., 2015. Mekanisme perlipatan en-echelon di Antiklinorium Rembang utara. In: Prosiding Seminar Nasional Kebumian Ke-8 Jurusan Teknik Geologi Fakultas Teknik Universitas Gadjah Mada, pp. 224–234. Yogyakarta, GEO41.

Husson, L., Boucher, F.C., Sarr, A.-C., Sepulchre, P., Cahyarini, S.Y., 2020. Evidence of Sundaland's subsidence requires revisiting its biogeography. J. Biogeogr. 47, 843–853.

Hyodo, M., Sunata, W., Susanto, E.E., 1992. A long-term geomagnetic excursion from Plio-Pleistocene sediments in Java. J. Geophys. Res. Solid Earth 97, 9323–9335.

Hyodo, M., Watanabe, N., Sunata, W., Susanto, E.E., Wahyono, H., 1993. Magnetostratigraphy of hominid fossil bearing formations in Sangiran and Mojokerto, Java. Anthropol. Sci. 101, 157–186.

Itihara, M., Watanabe, N., Kadar, D., Kumai, H., 1994. Quaternary stratigraphy of the hominid fossil bearing formations in the Sangiran area, Central Java. Courier Forschungs-Institut Senckenberg 171, 123–128.

Jacob, T., Curtis, G.H., 1971. Preliminary potassium-argon dating of early man in Java. Contributions of the University of California Archaeological research facility 12, 50.

Janssen, R., Joordens, J.C., Koutamanis, D.S., Puspaningrum, M.R., de Vos, J., Van Der Lubbe, J.H., Reijmer, J.J., Hampe, O., Vonhof, H.B., 2016. Tooth enamel stable isotopes of Holocene and Pleistocene fossil fauna reveal glacial and interglacial paleoenvironments of hominins in Indonesia. Quat. Sci. Rev. 144, 145–154.

Kelsey, H.M., Nelson, A.R., Hemphill-Haley, E., Witter, R.C., 2005. Tsunami history of an Oregon coastal lake reveals a 4600 yr record of great earthquakes on the Cascadia subduction zone. Geol. Soc. Am. Bull. 117, 1009–1032.

Kumai, H., 1985. Geology and stratigraphy of the Mojokerto area. Quaternary geology of the hominid fossil bearing formations in Java 55–61.

Laj, C., Channell, J.E., 2007. Geomagnetic excursions. Geomagnetism 5, 373–416.

Langbroek, M., Roebroeks, W., 2000. Extraterrestrial evidence on the age of the hominids from Java. J. Hum. Evol. 38, 595–600. https://doi.org/10.1006/jhev.1999.0394.

Lunt, P., 2013. The Sedimentary Geology of Java. Indonesian Petroleum Association.

Makaske, B., 2001. Anastomosing rivers: a review of their classification, origin and sedimentary products. Earth Sci. Rev. 53, 149–196.

Matsu'ura, S., Kondo, M., Danhara, T., Sakata, S., Iwano, H., Hirata, T., Kurniawan, I., Setiyabudi, E., Takeshita, Y., Hyodo, M., 2020. Age control of the first appearance datum for Javanese Homo erectus in the Sangiran area. Science 367, 210–214.

Mayr, E., 1950. Taxonomic categories in fossil hominids. In: Cold Spring Harbor Symposia on Quantitative Biology. Cold Spring Harbor Laboratory Press,

pp. 109–118.
Meikle, W.E., Parker, S.T., 1994. Naming Our Ancestors: an Anthology of Hominid Taxonomy. Waveland PressInc.
Miall, A.D., 2014. Fluvial Depositional Systems. Springer, Berlin.
Miall, A.D., 1996. The Geology of Fluvial Sediments. Springer, Berlin.
Morley, R.J., Morley, H.P., Swiecicki, T., 2016. Mio-pliocene Palaeogeography, Uplands and River Systems of the Sunda Region Based on Mapping within a Framework of Vim Depositional Cycles.
Morley, R.J., Morley, H.P., Zaim, Y., Huffman, O.F., 2020. Palaeoenvironmental setting of Mojokerto Homo erectus, the palynological expressions of Pleistocene marine deltas, open grasslands and volcanic mountains in East Java. J. Biogeogr. 47, 566–583.
Morwood, M.J., O'Sullivan, P., Susanto, E.E., Aziz, F., 2003. Revised age for Mojokerto 1, an early *Homo* erectus cranium from East Java, Indonesia. Aust. Archaeol. 57, 1–4. https://doi.org/10.1080/03122417.2003.11681757.
Mulder, T., Syvitski, J.P., 1995. Turbidity currents generated at river mouths during exceptional discharges to the world oceans. J. Geol. 103, 285–299.
Musliki, Saratman, 1996. A Late Pliocene Shallowing Upward Carbonate Sequence and its Reservoir Potential, Northeast Java Basin.
Nemec, W., 1990. Aspects of sediment movement on steep delta slopes. Coarse-grained deltas 10, 29–73.
Oppenoorth, 1932. Een Nieuwe Fossiele Mensch Van Java. Tijdschrift van het Koninklijk Nederlandsch Aardrijkskundig Genootschap, pp. 704–708.
Polhaupessy, A.A., 1990. Late Cenozoic Palynological Studies on Java (PhD Thesis). University of Hull.
Pons, L.J., Van Breemen, N., Driessen, P.M., 1982. Physiography of coastal sediments and development of potential soil acidity. Acid Sulfate Weathering 10, 1–18.
Pop et al., under review. Reconstructing the provenance of the hominin fossils from Trinil (Java, Indonesia) through an integrated analysis of the historical and recent excavations. Journal of Human Evolution..
Postma, G., Colella, A., Prior, D.B., 1990. Coarse-grained deltas. Int. Assoc. Sedimentol. Spec. Publ 10, 13–27.
Pringgoprawiro, H., 1983. Biostratigrafi Dan Paleogeografi Cekungan Jawa Timur Utara Suatu Pendekatan Baru. Disertasi ITB, Bandung.
Puspaningrum, M.R., van den Bergh, G.D., Chivas, A.R., Setiabudi, E., Kurniawan, I., 2020. Isotopic reconstruction of proboscidean habitats and diets on Java since the early Pleistocene: implications for adaptation and extinction. Quat. Sci. Rev. 228, 106007. https://doi.org/10.1016/j.quascirev.2019.106007.
Railsback, L.B., Gibbard, P.L., Head, M.J., Voarintsoa, N.R.G., Toucanne, S., 2015. An optimized scheme of lettered marine isotope substages for the last 1.0 million years, and the climatostratigraphic nature of isotope stages and substages. Quat. Sci. Rev. 111, 94–106. https://doi.org/10.1016/j.quascirev.2015.01.012.
Reinhold, T., 1937. Fossil duiatoms of the Neogene of Java and their zonal distribution. Verhandel. Geol. -Mijinbow. Geol. Ser. 12, 43–133.
Rizal, Y., Westaway, K.E., Zaim, Y., van den Bergh, G.D., Bettis, E.A., Morwood, M.J., Huffman, O.F., Grün, R., Joannes-Boyau, R., Bailey, R.M., Sidarto Westaway, M.C., Kurniawan, I., Moore, M.W., Storey, M., Aziz, F., Suminto Zhao, J., Aswan Sipola, M.E., Larick, R., Zonneveld, J.-P., Scott, R., Putt, S., Ciochon, R.L., 2020. Last appearance of Homo erectus at Ngandong, Java, 117,000–108,000 years ago. Nature 577, 381–385. https://doi.org/10.1038/s41586-019-1863-2.
Rogers, Kidwell, 2007. A Conceptual Framework for the Genesis and Analysis of Vertebrate Skeletal Concentrations. Bonebeds: Genesis, Analysis, and Paleobiological Significance. University of Chicago Press. Chicago 1–63.
Sarr, A.-C., Husson, L., Sepulchre, P., Pastier, A.-M., Pedoja, K., Elliot, M., Arias-Ruiz, C., Solihuddin, T., Aribowo, S., Susilohadi, 2019. Subsiding Sundaland. Geology 47, 119–122. https://doi.org/10.1130/G45629.1.
Sartono, S., 1981. The age of Homo modjokertensis. Mod. Quaternary Res. SE Asia 6, 91–102.
Satyana, A.H., 2007. Central Java, Indonesia—A "Terra Incognita" in Petroleum Exploration: New Considerations on the Tectonic Evolution and Petroleum Implications.
Satyana, A.H., Armandita, C., 2004. Deepwater Plays of Java, Indonesia: Regional Evaluation on Opportunities and Risks.
Satyana, A.H., Erwanto, E., Prasetyadi, C., 2004. Rembang-Madura-Kangean-Sakala (RMKS) Fault Zone, East Java Basin: the Origin and Nature of A Geologic Border. Proc. IAGI, 33rd., Ann. Conv. And Exh., Bandung.
Sellés-Martínez, J., 1996. Concretion morphology, classification and genesis. Earth Sci. Rev. 41, 177–210.
Sémah, A.-M., Sémah, F., 2012. The rain forest in Java through the Quaternary and its relationships with humans (adaptation, exploitation and impact on the forest). Quat. Int. 249, 120–128. https://doi.org/10.1016/j.quaint.2011.06.013.
Sémah, A.-M., Sémah, F., Djubiantono, T., Brasseur, B., 2010. Landscapes and hominids' environments: changes between the lower and the early middle Pleistocene in Java (Indonesia). Quat. Int. 223, 451.
Smyth, H., Hall, R., Hamilton, J., Kinny, P., 2005. East Java: cenozoic basins, volcanoes and ancient basement. In: Proceedings of the Indonesian Petroleum Association, 30th Annual Convention. Indonesian Petroleum Association, pp. 251–266.
Smyth, H.R., Hall, R., Nichols, G.J., 2008. Cenozoic volcanic arc history of East Java, Indonesia: the stratigraphic record of eruptions on an active continental margin. Spec. Pap. Geol. Soc. Am. 436, 199.
Storm, P., 1994. De morfologie van Homo modjokertensis. CRANIUM 11, 97–102.
Susilohadi, 1995. Late Tertiary and Quaternary Geology of the East Java Basin, Indonesia (PhD Thesis). University of Wollongong.
Swisher, C.C., Curtis, G.H., Jacob, T., Getty, A.G., Suprijo, A., Widiasmoro, 1994. Age of the earliest known hominids in Java, Indonesia. Science 263, 1118–1121. https://doi.org/10.1126/science.8108729.
Tebbens, L.A., Veldkamp, A., Westerhoff, W., Kroonenberg, S.B., 1999. Fluvial incision and channel downcutting as a response to Late-glacial and Early Holocene climate change: the lower reach of the River Meuse (Maas), The Netherlands. J. Quat. Sci.: Published for the Quaternary Research Association 14, 59–75.
Trooster, 1937. Nota betreffende Ir. J. Duyfjes "Zur Geologie und Statigraphie ders Kendenggebietes zwischen Trinil und Soerabaia. Bataafse Internationale Petroleum Maatschappij.
Tucker, M.E., 1985. Shallow-marine carbonate facies and facies models. Geological Society, London, Special Publications 18, 147–169.
van Bemmelen, R.W., 1949. The Geology of Indonesia. 1, A. General Geology of Indonesia and Adjacent Archipelagoes. US Government Printing Office.
Van den Bergh, G.D., 1999. The Late Neogene elephantoid-bearing faunas of Indonesia and their palaeozoogeographic implications. Scripta Geol. 117, 1–419.
Van den Bergh, G.D., de Vos, J., Sondaar, P.Y., 2001. The Late Quaternary palaeogeography of mammal evolution in the Indonesian Archipelago. Palaeogeogr. Palaeoclimatol. Palaeoecol. 171, 385–408.
Van Gorsel, J.T., Troelstra, S.R., 1981. Late Neogene planktonic foraminiferal biostratigraphy and climatostratigraphy of the Solo River section (Java, Indonesia). Marine Micropaleontology 6, 183–209. https://doi.org/10.1016/0377-8398(81)90005-0.
Veldkamp, A., Tebbens, L.A., 2001. Registration of abrupt climate changes within fluvial systems: insights from numerical modelling experiments. Global Planet. Change 28, 129–144.
Von Koenigswald, G.H.R., 1936. Ein fossiler hominide aus dem Altpleistocan Ostjavas. De Ingenieur ned.-Indie 4, 149–157.
Von Koenigswald, G.H.R., 1935. Die saugetierfaunen javas. Proc. Kon. Akad.v. Wetensch, Amsterdam 38, 188–198.
Von Koenigswald, G.H.R., 1934. Zur Stratigraphie des Javanischen Pleistocan. De Ingenieur in Nederlands-Indie 1, 185–201.
Zahirovic, S., Flament, N., Dietmar Müller, R., Seton, M., Gurnis, M., 2016. Large fluctuations of shallow seas in low-lying S outheast A sia driven by mantle flow. G-cubed 17, 3589–3607.
Zavala, C., 2020. Hyperpycnal (over density) flows and deposits. J. Palaeogeogr. 9, 1–21.
Zolitschka, B., Francus, P., Ojala, A.E., Schimmelmann, A., 2015. Varves in lake sediments–a review. Quat. Sci. Rev. 117, 1–41.